Articles

Synthesis, Biological Activity, and SARs of Pyrrolobenzoxazepine Derivatives, a New Class of Specific "Peripheral-Type" Benzodiazepine Receptor Ligands[1]

Giuseppe Campiani,[†] Vito Nacci,*[,†] Isabella Fiorini,[†] Maria P. De Filippis,[†] Antonio Garofalo,[†] Silvia M. Ciani,[†] Giovanni Greco,[‡] Ettore Novellino,[‡] D. Clive Williams,[§] Daniela M. Zisterer,[§] Margaret J. Woods,[§] Camelia Mihai,[§] Cristina Manzoni,[||] and Tiziana Mennini[||]

Dipartimento Farmaco Chimico Tecnologico, Universita' di Siena, Banchi di Sotto 55, 53100 Siena, Italy, Istituto di Ricerche Farmacologiche "Mario Negri", via Eritrea 62, 40126 Milano, Italy, Department of Biochemistry, Trinity College, Dublin 2, Ireland, and Dipartimento di Chimica Farmaceutica e Tossicologica, Universita' di Napoli "Federico II", via D. Montesano 49, 80131 Napoli, Italy

Received April 1, 1996[⊗]

The "peripheral-type" benzodiazepine receptor (PBR) has been reported to play a role in many biological processes. We have synthesized and tested a novel series of PBR ligands based on a pyrrolobenzoxazepine skeleton, in order to provide new receptor ligands. Several of these new compounds proved to be high affinity and selective ligands for PBR, and benzoxazepines **17f** and **17j** were found to be the most potent ligands for this receptor to have been identified to date. The SAR and the molecular modeling studies detailed herein delineated a number of structural features required for improving affinity. Some of the ligands were employed as "molecular yardsticks" to probe the spatial dimensions of the lipophilic pockets L1 and L3 in the PBR cleft and to determine the effect of occupation of L1 and L3 with respect to affinity, while other C-7 modified analogues provided information specifically on the hydrogen bonding with a putative receptor site H1. The new pyrrolobenzoxazepines were tested in rat cortex, a tissue expressing high density of mitochondrial PBR, and exhibited IC_{50} and K_i values in the low nanomolar or subnanomolar range, as measured by the displacement of [^{3}H]PK 11195 binding. A subset of the highest affinity ligands was also found to have high affinities for [^{3}H]PK 11195 and [^{3}H]Ro 5-4864 binding in rat adrenal mitochondria. All the ligands in this subset are stimulators of steroidogenesis having similar potency and extent of stimulation as PK 11195 and Ro 5-4864 of steroidogenesis in the mouse Y-1 adrenocortical cell line.

Introduction

The "peripheral-type" benzodiazepine receptor (PBR) is pharmacologically distinct from the central-type benzodiazepine receptor (CBR) associated with GABA-regulated chloride channels in the central nervous system (CNS).[2−6] Although the PBR has been found within the CNS,[4,7,8] mainly in astrocytes, it is abundant in peripheral tissues, including kidney,[9,10] heart,[11,12] erythrocytes,[13,14] and particularly in endocrine tissues (testis and adrenal cortex).[15] This receptor is characterized by high affinity binding of isoquinolines, such as PK 11195 (**1**),[16] of benzodiazepines, such as Ro 5-4864 (**2**),[7] of imidazopyridines (alpidem **3**),[17] of indole derivatives (**4**),[18] and of benzothiazepines (**5**).[19] The PBR has been characterized as being predominantly associated with mitochondria, specifically on the outer mitochondrial membrane.[20] Physiologically, the PBR may be involved in regulatory mechanisms that vary among the different tissues in which it is present. PBR-mediated effects include calcium homeostasis,[21] lipid metabolism,[22] mitochondrial oxidation,[23] inhibition of cell proliferation,[24] and alteration of protooncogene expression,[25] but the involvement of PBR in the regulation of steroid biosynthesis is probably the most intriguing aspect of its biological role with respect to possible therapeutic applications.[26] Steroid hormones, such as pregnenolone, 3α-hydroxy-5α-pregnan-20-one (3α-OH-DHP), dehydroepiandrosterone, and 3α,21-dihydroxy-5α-pregnan-20-one (THDOC) are mainly produced peripherally by the adrenal gland. It has been recently demostrated that the synthesis of these steroids may also occur within the CNS in glial cells.[27] Recent reports suggest that the PBR, located in the outer mitochondrial membrane in glial and peripheral endocrine cells, plays a crucial role in steroid biosynthesis[28−32] by regulating the rate-limiting translocation of cholesterol from the outer to the inner mitochondrial membrane before its transformation by cytochrome $P450_{scc}$ into pregnenolone which is further metabolized to other bioactive hormones. DBI, an endogenous PBR ligand abundant in steroidogenic cells, and synthetic ligands, such as PK 11195, Ro 5-4864, and FGIN-1-27, facilitate the transport of cholesterol inside the mitochondria, and are found to increase the rate of pregnenolone synthesis in mitochondrial fractions in Leydig and adrenocortical cell lines.[33−35] Adrenally derived or centrally produced steroid hormones (e.g. 3α-OH-DHP, pregnenolone, and THDOC), can influence neuronal excitability *via* different targets. These steroids can bind with high affinity a recognition site coupled to the $GABA_A$−benzodiaz-

* To whom correspondence should be addressed.
[†] Dipartimento Farmaco Chimico Tecnologico, Universita' di Siena.
[‡] Dipartimento di Chimica Farmaceutica, Universita' di Napoli "Federico II".
[§] Department of Biochemistry, Trinity College, Dublin.
[||] Istituto di Ricerche Farmacologiche "Mario Negri", Milano.
[⊗] Abstract published in *Advance ACS Abstracts,* August 1, 1996.

S0022-2623(96)00251-8 CCC: $12.00

Chart 1

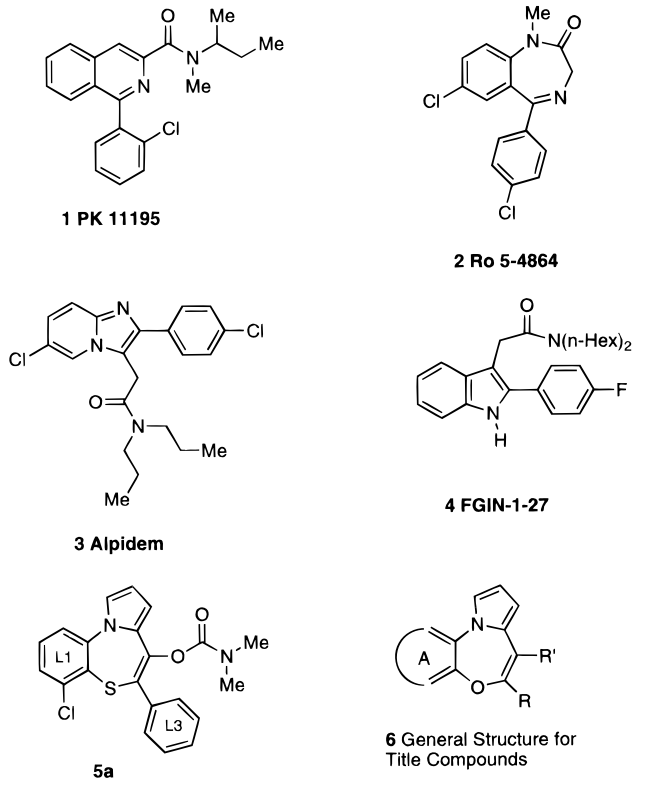

Scheme 1

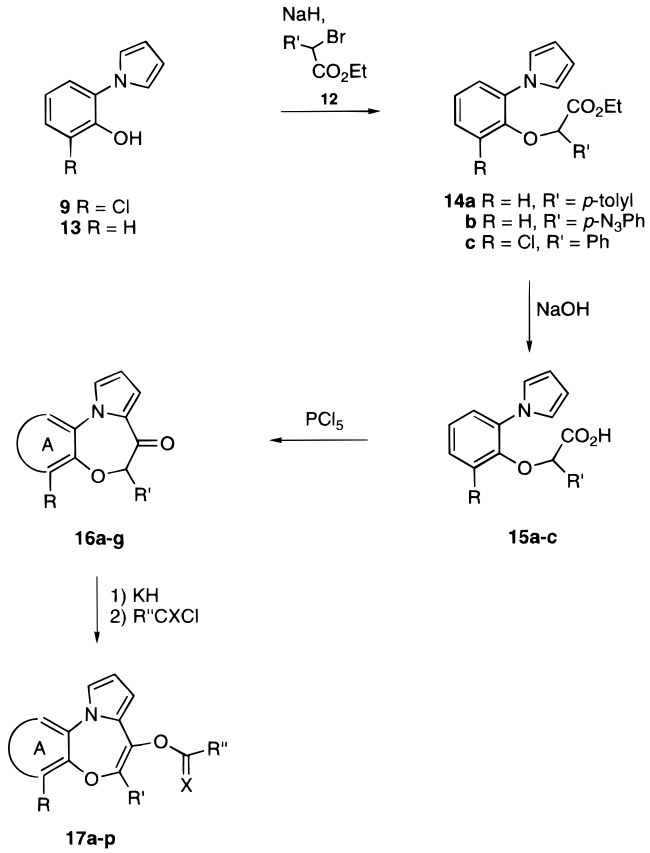

epine receptor complex and can modulate the action of glutamate on NMDA receptors.[36−38] Their behavioral properties are probably the consequence of these interactions.[39] Thus PBR could represent an alternative site for an indirect modulation of GABAergic and glutamatergic neurotransmission by increasing the level of peripherally or centrally derived steroid hormones, followed by their $GABA_A$ and NMDA receptor modulation. In this article we present a further development in our research on novel PBR ligands. We detail herein the synthesis of pyrrolobenzoxazepine derivatives **6** (Chart 1) and their structure−activity relationships (SARs) for PBR affinity associated with variation of the substituents on the heterocyclic system. Several of these new compounds bind the PBR with both high affinity and specificity, and benzoxazepines **17f** and **17j** were found to be the most potent ligands for this receptor to have been identified to date. A subset of ligands with high affinity in brain was further tested for their ability to displace [^{3}H]PK 11195 and [^{3}H]Ro 5-4864 from the rat adrenal receptor and for their potencies to modulate steroid biosynthesis in a Y-1 adrenocortical cell line, and all were found to stimulate pregnenolone formation with potencies equivalent to PK 11195 and Ro 5-4864. The SARs developed in the present study are discussed in the light of a previously reported pharmacophore model,[40] schematically represented in Chart 2. According to this model, a hydrogen bond-donating function (H1) and two lipophilic pockets (L1 and L3) within the receptor binding site are available to our ligands. The presence of an additional lipophilic region (L4) has been deduced from analysis of the SARs relative to the newly investigated pyrrolobenzoxazepines.

Chemistry

The new pyrrolobenzoxazepinones **16a**−**c** were synthesized as shown in Scheme 1, according to the procedure utilized to prepare already known **16d**−**g**,[41] starting from the appropriate 1-arylpyrrole. 1-(3-Chloro-2-hydroxyphenyl)pyrrole (**9**) was synthesized following the procedure illustrated in eq 1,[42] while **13** was prepared according to reference 43. The esters **14a**−**c** were obtained in good yield starting from **9** and **13** by

Chart 2. H1 is a Hydrogen Bond Donor Site on the Receptor Protein. L1, L3, and L4 are Lipophilic Pockets in the Protein at the Binding Site

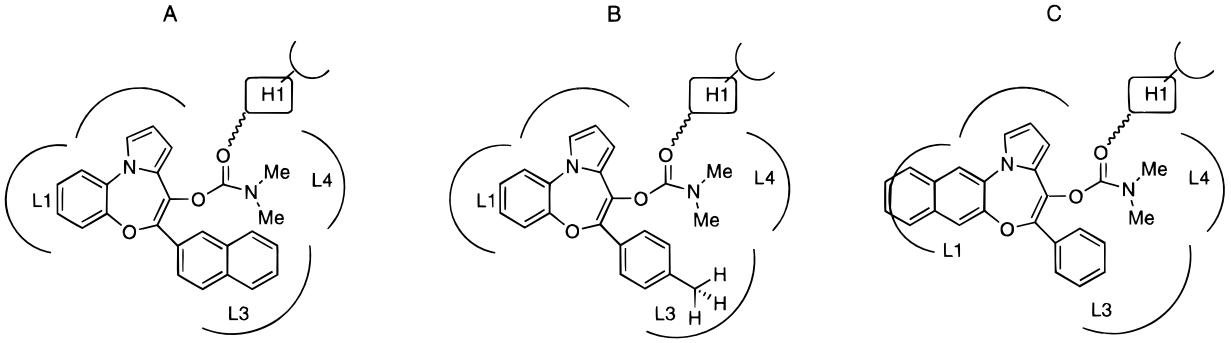

Table 1. Physical Data for Compounds **8**–**22**

compd	A	X	R	R′	R″	% yield[a]	mp (°C)	recryst solvent	formula	analysis[b]
8[c]						45	70–71	EtOAc	$C_6H_4ClNO_3$	C,H,N
9						76	64–65	hexanes	$C_{10}H_8ClNO$	C,H,N
11a						74	102–104	EtOAc/hexanes	$C_8H_7N_3O_2$	C,H,N
12a						40	–	–	$C_{10}H_{10}BrN_3O_2$	C,H,N
12b						53	–	–	$C_{11}H_{13}BrO_2$	C,H,N
14a						53	–	–	$C_{21}H_{21}NO_3$	C,H,N
14b						93	–	–	$C_{20}H_{17}N_4O_3$	C,H,N
14c						56	–	–	$C_{20}H_{18}ClNO_3$	C,H,N
15a						94	140–142	hexanes	$C_{19}H_{17}NO_3$	C,H,N
15b						95	130 (d)	EtOAc/hexanes	$C_{18}H_{14}N_4O_3$	C,H,N
15c						98	220–221	hexanes	$C_{18}H_{14}ClNO_3$	C,H,N
16a	benzo		H	*p*-tolyl		74	79–81	EtOH	$C_{19}H_{15}NO_2$	C,H,N
16b	benzo		H	*p*-N_3-phenyl		40	113–115	EtOAc/hexanes	$C_{18}H_{12}N_4O_2$	C,H,N
16c	benzo		Cl	phenyl		60	122–123	hexanes	$C_{18}H_{12}ClNO_2$	C,H,N
16d[d]	benzo		H	phenyl		–	–	–	–	
16e[d]	benzo		H	2-naphthyl		–	–	–	–	
16f[d]	[2,3]naphtho		H	phenyl		–	–	–	–	
16g[d]	benzo		H	ethyl		–	–	–	–	
17a	benzo	O	H	ethyl	Me	67	–	–	$C_{16}H_{15}NO_3$	C,H,N
17b	benzo	O	H	ethyl	$N(Me)_2$	73	104–106	hexanes	$C_{17}H_{18}N_2O_3$	C,H,N
17c	benzo	O	H	phenyl	Me	78	118–119	EtOH	$C_{20}H_{15}NO_3$	C,H,N
17d	benzo	O	H	phenyl	C_6H_{11}	83	101–102	hexanes	$C_{25}H_{23}NO_3$	C,H,N
17e	benzo	O	H	phenyl	$N(Me)_2$	66	151–152	EtOH	$C_{21}H_{18}N_2O_3$	C,H,N
17f	benzo	O	H	phenyl	$N(Et)_2$	73	61–63	hexanes	$C_{23}H_{22}N_2O_3$	C,H,N
17g	benzo	S	H	phenyl	$N(Et)_2$	59	150–151	hexanes	$C_{23}H_{22}N_2O_2S$	C,H,N
17h	benzo	O	H	*p*-tolyl	Me	60	129–130	EtOH	$C_{21}H_{17}NO_3$	C,H,N
17i	benzo	O	H	*p*-tolyl	$N(Me)_2$	56	154–155	hexanes/ethyl ether	$C_{22}H_{20}N_2O_3$	C,H,N
17j	benzo	O	H	*p*-tolyl	$N(Et)_2$	72	130–132	hexanes/EtOAc	$C_{24}H_{24}N_2O_3$	C,H,N
17k	benzo	O	H	2-naphthyl	Me	69	157–158	EtOH	$C_{24}H_{17}NO_3$	C,H,N
17l	benzo	O	H	2-naphthyl	$N(Me)_2$	65	173–175	EtOH	$C_{25}H_{20}N_2O_3$	C,H,N
17m	benzo	O	H	*p*-N_3-phenyl	$N(Me)_2$	67	–	–	$C_{21}H_{17}N_5O_3$	C,H,N
17n	benzo	O	Cl	phenyl	$N(Me)_2$	65	175–177	hexanes	$C_{21}H_{17}ClN_2O_3$	C,H,N
17o	[2,3]naphtho	O	H	phenyl	Me	58	164–165	EtOH	$C_{24}H_{17}NO_3$	C,H,N
17p	[2,3]naphtho	O	H	phenyl	$N(Me)_2$	53	189–191	hexanes	$C_{25}H_{20}N_2O_3$	C,H,N
19						63	119–120	hexanes/EtOAc	$C_{20}H_{15}NO_3$	C,H,N
20						58	108–110	EtOH	$C_{20}H_{15}NO_2$	C,H,N
21						90	88–89	hexanes	$C_{19}H_{15}NO_2$	C,H,N
22						83	69–71	hexanes	$C_{21}H_{17}NO_3$	C,H,N

[a] Yields refer to isolated and purified materials. [b] All the compounds were analyzed within ±0.4% of the theoretical values. [c] Reference 42 (mp 66–70 °C, 20% yield). [d] Reference 41.

treatment with sodium hydride and the appropriate ethyl α-bromoarylacetate (**12**), **12a**,**b** in turn prepared as shown in eq 2.[44] Hydrolysis of esters **14a**–**c** with

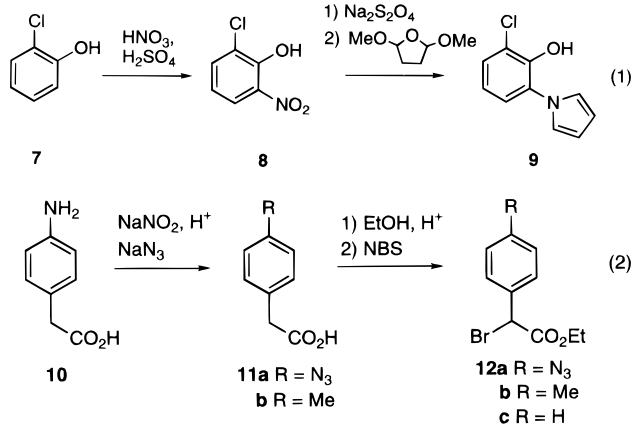

sodium hydroxide (**15a**–**c**) followed by intramolecular cyclization using phosphorus pentachloride gave the benzoxazepinones **16a**–**c**. Treatment of the corresponding potassium enolates of **16a**–**g** with selected acyl chlorides finally yielded the desired oxazepines **17a**–**p** (see Table 1). The C-7 modified oxazepines **19**, **20**, and **22** were synthesized starting from **16d** (see Scheme 2) which was transformed to the ester derivative **19** by exposure of its triflate intermediate **18** to carbon monoxide and methanol in presence of tetrakis(triphenylphosphine)palladium.[45] The ketone **20** was

Scheme 2

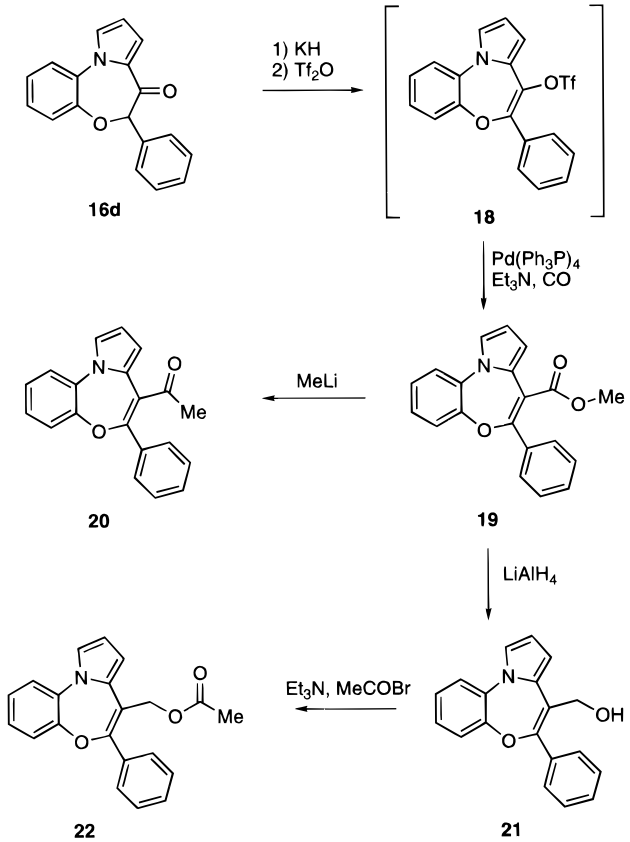

Table 2. Receptor Binding Affinity of Compounds **17a−p**

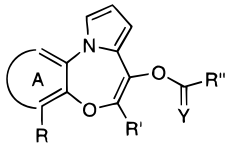

17a-p

compd	A	Y	R	R′	R″	IC_{50} (nM)[a] (±SEM)	K_i (nM)[a] (±SEM)
17a	benzo	O	H	ethyl	Me	>5000	
17b	benzo	O	H	ethyl	$N(Me)_2$	589 ± 81	230 ± 32
17c	benzo	O	H	phenyl	Me	12.1 ± 1	4.7 ± 0.4
17d	benzo	O	H	phenyl	C_6H_{11}	81.9 ± 20	32.0 ± 8
17e	benzo	O	H	phenyl	$N(Me)_2$	5.1 ± 0.3	2.0 ± 0.12
17f	benzo	O	H	phenyl	$N(Et)_2$	0.68 ± 0.18	0.26 ± 0.07
17g	benzo	S	H	phenyl	$N(Et)_2$	3.8 ± 1.3	1.5 ± 0.5
17h	benzo	O	H	*p*-tolyl	Me	2.3 ± 0.5	0.91 ± 0.2
17i	benzo	O	H	*p*-tolyl	$N(Me)_2$	1.3 ± 0.2	0.52 ± 0.08
17j	benzo	O	H	*p*-tolyl	$N(Et)_2$	0.94 ± 0.06	0.36 ± 0.02
17k	benzo	O	H	2-naphthyl	Me	76.6 ± 7	30.0 ± 2.7
17l	benzo	O	H	2-naphthyl	$N(Me)_2$	6.0 ± 1.7	2.4 ± 0.7
17m	benzo	O	H	*p*-N_3-phenyl	$N(Me)_2$	3.6 ± 0.5	1.4 ± 0.2
17n	benzo	O	Cl	phenyl	$N(Me)_2$	1.3 ± 0.1	0.51 ± 0.04
17o	[2,3]naphtho	O	H	phenyl	Me	278 ± 19	108.0 ± 7
17p	[2,3]naphtho	O	H	phenyl	$N(Me)_2$	37.3 ± 9.4	14.5 ± 3.6
5a[b]						4.0 ± 1	1.8 ± 0.4
PK 11195						2.0 ± 0.1	0.78 ± 0.04

[a] The concentration of the tested compounds that inhibited [^{3}H]PK 11195 binding to rat cortex homogenate by 50% (IC_{50}) was determined by log-probit analysis with 6 concentrations of the displacers, each performed in triplicate. Values are the mean ± SE of at least three separate experiments, performed in triplicate. [b] Reference 19b.

Table 3. Comparison of PBR Binding Affinity of Compounds Modified at C-7

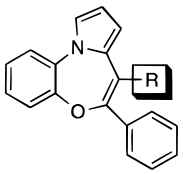

compd	R	IC_{50} (nM)[a] (±SEM)	K_i (nM)[a] (±SEM)
17c	OCOMe	12.1 ± 1.0	4.7 ± 0.4
17e	$OCON(Me)_2$	5.1 ± 0.3	2.0 ± 0.12
17f	$OCON(Et)_2$	0.68 ± 1.8	0.26 ± 0.07
17g	$OCSN(Et)_2$	3.8 ± 1.3	1.5 ± 0.5
19	CO_2Me	148 ± 39	57.8 ± 15
20	COMe	64.6 ± 39	25.2 ± 15
22	CH_2OCOMe	1930 ± 610	754 ± 237
PK 11195		2.0 ± 0.1	0.78 ± 0.04

[a] The concentration of the tested compounds that inhibited [^{3}H]PK 11195 binding to rat cortex homogenate by 50% (IC_{50}) was determined by log-probit analysis with 6 concentrations of the displacers, each performed in triplicate. Values are the mean ± SE of at least three separate experiments performed in triplicate.

obtained by treatment of **19** with methyllithium at 0 °C[46] (in these conditions from the reaction mixture was recovered only 10% of the corresponding tertiary alcohol), while the ester **22** was synthesized by esterification with acetyl bromide of **21**, in turn prepared by lithium aluminum hydride reduction of **19** (see Table 1).

Biological Studies

The affinities of the new pyrrolobenzoxazepine derivatives for the PBR in rat cortex homogenate are illustrated in Tables 2 and 3. For sake of comparison the affinities of a set of previously described benzothiazepines are reported in Table 4. The binding data presented in Tables 2 and 3 represent the ability of the tested compounds to displace [^{3}H]PK 11195 from the receptor protein. Binding data of PK 11195 is also included. Benzoxazepine **17i**, one of the most potent PBR ligands, was found to be inactive on the chloride channel associated to $GABA_A$ receptor and on CBR, as indicated by its lack of inhibition of [^{35}S]TBPS and [^{3}H]-flunitrazepam binding, respectively, to rat cerebral membranes, even at the highest concentration tested (10^{-5} M).[19a] This result suggests that the chemical structures under study are selective for PBR and do not interact with CBR. Binding studies using [^{3}H]PK 11195 and [^{3}H]Ro 5-4864 were also carried out using rat adrenal mitochondria for compounds **5a**, **17e**, **17h**−**j**, and **17l**,**m**. Rat adrenals were chosen as an additional source of tissue since they have previously been reported to contain a very high density of high affinity PBR binding sites[15] with identical binding properties to the brain receptor. The compounds tested in adrenal mitochondria were found to exhibit significant binding affinity (K_i values range from 0.8−4.8 nM) for the PBR. In fact these K_i values are similar to the K_d values obtained for [^{3}H]PK 11195 and [^{3}H]Ro 5-4864 binding (1.5 and 2.2 nM, respectively) (Table 5). A subset of PBR ligands showing high affinity for the PBR have been examined for their ability to stimulate pregnenolone formation in Y-1 cells.

Both PK 11195 and Ro 5-4864 have previously been shown to maximally stimulate steroid production by 2-fold in Y-1 cells[33,35] and to elicit similar effects in MA10 Leydig cells,[47] C6-2B glioma cells[48] and in freshly isolated rat adrenal cells,[33] albeit at much higher concentrations than theoretically required to saturate the PBR. All the compounds tested stimulated steroidogenesis in a concentration-dependent manner with similar concentration dependencies to PK 11195 and Ro 5-4864. In order to make a direct comparison of efficacies, all the compounds were tested in the same experiment at a single concentration (40 μM). At the same time clonazepam, a ligand selective for the central-

Table 4. Receptor Binding Affinity of Compounds **5a**−**g**

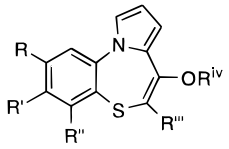

5a-g

compd	R	R′	R″	R‴	R^{iv}	IC_{50} (nM) (±SEM)	K_i (nM) (±SEM)	ref
5a	H	H	Cl	phenyl	$CON(Me)_2$	4.0 ± 1	1.8 ± 0.4	19b
5b	H	H	H	phenyl	COMe	20 ± 2	7.6 ± 0.7	19a
5c	H	H	H	phenyl	$CO(NMe)_2$	9.0 ± 1	3.5 ± 0.4	19a
5d	H	H	H	4′-Cl-phenyl	COMe	30 ± 3	11.7 ± 1.1	19b
5e	Me	H	H	phenyl	COMe	675 ± 75	263 ± 29	19b
5f	H	Me	H	phenyl	COMe	112 ± 21	44 ± 8	19b
5g	H	H	H	4′-MeO-phenyl	CO-3′-pyridyl	$>10^5$		19a
PK 11195						2.0 ± 0.1	0.78 ± 0.04	

Table 5. K_i Values for Tested Compounds for Displacing [^{3}H]Ro 5-4864 and [^{3}H]PK 11195 from the Rat Adrenal PBR

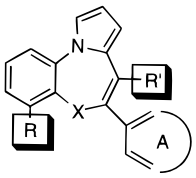

					K_i (nM) (±SEM)[a]	
compd	A	R	R′	X	[^{3}H]Ro 5-4864	[^{3}H]PK 11195
5a	phenyl	Cl	$OCON(Me)_2$	S	2.6 ± 0.5	2.5 ± 0.6
17e	phenyl	H	$OCON(Me)_2$	O	0.8 ± 0.3	1.0 ± 0.2
17h	*p*-tolyl	H	OCOMe	O	1.7 ± 3.2	2.8 ± 1.0
17i	*p*-tolyl	H	$OCON(Me)_2$	O	1.3 ± 1.0	1.1 ± 0.1
17j	*p*-tolyl	H	$OCON(Et)_2$	O	1.9 ± 0.5	1.9 ± 0.4
17l	2-naphthyl	H	$OCON(Me)_2$	O	1.8 ± 0.3	1.9 ± 0.7
17m	*p*-N_3-phenyl	H	$OCON(Me)_2$	O	3.6 ± 0.8	4.8 ± 1.2

[a] K_i values represent the mean ± SEM of three determinations. The K_i values and errors for each compound were generated by the use of the computer programmes EBDA and LIGAND.

type $GABA_A$/benzodiazepine receptor, did not elicit any stimulatory effect at this concentration. This suggests that the stimulatory effect of the tested compounds on steroid biosynthesis may be mediated through the PBR (Table 6).

Preliminary studies have been carried out in order to assess the potential of **17m** as a photoaffinity ligand for the PBR. Whereas light-dependent irreversible inhibition of the binding of [^{3}H]PK 11195 and [^{3}H]Ro 5-4864 to rat adrenal mitochondria was observed, the inhibition was not blocked by the presence of Ro 5-4864 and PK 11195. Further work is necessary to expand these findings and to assess the receptor site involved in the binding of the presented compounds.

Computational Chemistry

Molecular modeling studies were performed to assist the design of the investigated compounds and the development of structure−affinity relationships. Semiempirical quantum-mechanics and molecular mechanics methods were employed in combination to identify pharmacophore-consistent conformations of some structurally representative pyrrolobenzoxazepines. Crystal structures determined by us[40] or available from the Cambridge Structural Database (CSD)[49] were used to compare experimental versus theoretical geometries. Protocols and outcomes of the computational studies are described in the Experimental Section and Results and Discussion, respectively.

Results and Discussion

A comparison of the IC_{50} values relative to the three pairs of isosteric pyrrolobenzothiazepines (Table 4) and pyrrolobenzoxazepines listed in Tables 2 and 3 (**17c** *vs* **5b**, **17e** *vs* **5c** and **17n** *vs* **5a**) reveals that replacement of the endocyclic sulfur (S5) with an oxygen (O5) increases affinities by 2−3 fold. This order of magnitude is not large enough to propose an involvement of the O5 atom in a hydrogen bond with the receptor. It is well known that oxygen is a much better hydrogen bond acceptor than sulfur in the sp^3 hybridization state,[50,51] and hence differences in potency should be more evident if O5 was actually engaged in this type of interaction. It is possible that the extra affinity of the pyrrolobenzoxazepines originates from an improved stereoelectronic complementarity between the O5 and a specific subsite of the receptor. Alternatively, modifications of C−S(O) distances and C−S(O)−C angle would introduce changes in the overall 3D arrangement of the tricyclic system and thus indirectly favor interactions involving other parts of the ligand.

Figure 1 shows the hypothetical active conformations of Ro 5-4864, **17c**, and **5d** aligned about the L1, L3, and H1 pharmacophoric elements (compounds **17c** and **5d** were chosen as representatives of the two isosteric series). Table 7 summarizes the pharmacophore-consistent conformations of all the modeled structures.

According to the pharmacophoric distances listed in Table 7 and as illustrated in Figure 1, the pyrrolobenzoxazepines are more superimposable on the L1, L3, and H1 points of Ro 5-4864 than are their sulfurated isosteres. One may speculate that the beneficial effect of the S5/O5 replacement originates from a more precise orientation of the anchoring functions into the receptor cavity. Despite these geometric differences, it seems reasonable to assume that pyrrolobenzoxazepines and pyrrolobenzothiazepines share a similar binding mode at the PBR. This assumption is supported by parallel structure−affinity relationships in the two series. Specifically, affinity is enhanced by conversion of the 7-acetoxy into a 7-(dimethylcarbamoyl)oxy group (**17c** *vs* **17e** and **5b** *vs* **5c**) or by the presence of a chlorine at the 4-position (**17e** *vs* **17n** and **5c** *vs* **5a**). The binding to the receptor is weakened by substitutions at the 2- and 3-positions (**17e** *vs* **17p** and **5b** *vs* **5e** and **5f**).

Compounds **17a** and **17b**, both bearing an ethyl in

Table 6. Stimulatory Effect on Steroid Biosynthesis of Y-1 Cells

compd	Pregnenolone production (ng/2h/3x10^5 cells)[a]
Control	21.9 ± 0.9
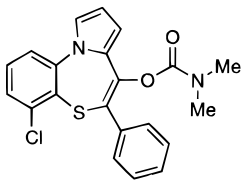 **5a**	29.3 ± 1.1
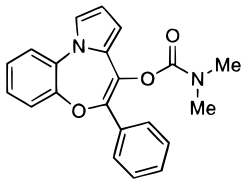 **17e**	33.7 ± 1.2
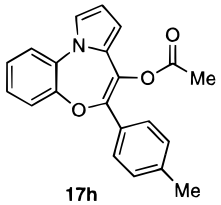 **17h**	29.3 ± 0.9
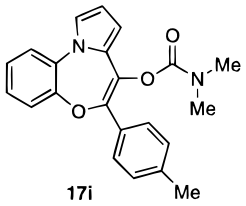 **17i**	38.4 ± 1.8
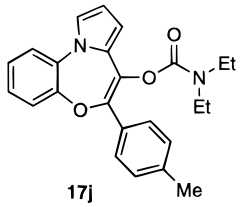 **17j**	40.4 ± 1.1
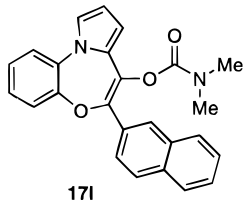 **17l**	27.5 ± 1.5
PK 11195	33.2 ± 1.2
Ro 5-4864	29.5 ± 0.5
Clonazepam	22.1 ± 0.7

[a] The values represent the mean ± SEM of three experiments. For comparison purpose the effect of PK 11195, Ro 5-4864, and Clonazepam on steroid production at 40 μM concentration is also included.

place of an aryl group at the 6-position, were synthesized to verify whether the interaction about the L3 site is actually needed for nanomolar affinity as previously postulated by us.[40] The hydrophobic constants π of the ethyl and phenyl substituents are 1.02 and 1.96, respectively, within the classical reference system of benzene.[52] From the IC_{50} values of the pairs **17a**/**17c** and **17b**/**17e** it can be concluded that halving the lipophilicity of the 6-substituent reduces affinity by more than a 100 fold. These data confirm the key role of the L3 site in the binding to the PBR. By introducing lipophilic substituents at the 4′-position of the 6-phenyl ring we attempted to exploit the lipophilic interaction at the L3 receptor region. Indeed, methylation at the 4′-position of **17c** and **17e** afforded **17h** and **17j**, respectively, which turned out to be 4−5 times more potent. The higher affinity of the 4′-azido derivative **17m**, compared with **17e**, might similarly be the consequence of a more favorable hydrophobic interaction at the L3 site (the π values[52] of the methyl and azido groups are 0.56 and 0.46, respectively). When the same 4′-methyl group was introduced in the structure of **17f**, the affinity of the resulting compound (**17j**) was comparable to that of **17f** in rat brain. Clearly, in this case we cannot make use of a simple additive model of ligand−receptor interaction to explain why parallel structural modifications do not produce parallel changes in affinity. Replacement of the 6-phenyl with the 6-(2-naphthyl) group (**17k**,**l** *vs* **17c**,**e**), and of the benzo-fused ring with a [2,3]naphtho-fused ring (**17o**,**p** *vs* **17c**,**e**) was realized to probe the dimensions of the L1 and L3 sites. While **17k** and **17l** retained a nanomolar affinity, although lower than that of the parent compounds **17c**,**e**, the compounds **17o**,**p** showed an affinity 4- to 5-fold lower, indicating that 2- and 3- positions of the benzo-fused ring of **17c**,**e** are located in close proximity of the steric boundaries of the L1 region, and that the latter region cannot tolerate an additional large benzo-fused ring which extends to an area of negative interaction (**17o**,**p**) (Chart 2).

Comparison of a C-7 Aroyl (5g) with a C-7 Cycloalkanoyl (17d) Group. According to recently published crystallographic and theoretical studies[19,40] the inactivity of several 7-aroyloxy benzothiazepines was thought to depend on steric and/or electrostatic repulsive interactions involving their aryl moieties and a specific site of the PBR. Such aryl groups might be in fact too bulky and/or too electronegative to fit into the receptor cavity. Addressing this issue might be important for delineating the physicochemical nature of the receptor region complementary to the 7-substituent of either pyrrolobenzothiazepines or pyrrolobenzoxazepines. Compound **17d**, featuring the encumbering nonaromatic 7-cyclohexylcarbonyloxy side chain, was therefore synthesized and tested. The affinity of **17d** is about 7 times lower than its reference analogue **17c** whereas, in the pyrrolobenzothiazepine series, the insertion of a 7-aroyloxy group led to a total loss of affinity (see **5g** in Table 4). Figure 2 shows **17d** and **5g** in their pharmacophore-consistent conformation (geometries are described in Table 7) along with their electrostatic potentials contoured at −5 kcal/mol. It should be noted that the side chains of the two molecules are rather similar in shape but quite different in their electrostatic properties. Taken together, these observations suggest that the disruptive effect of a 7-aroyloxy group should be mainly ascribed to an electrostatic repulsive interaction occurring between the π-conjugat-

Table 7. Geometries of Pharmacophore-Consistent Conformations

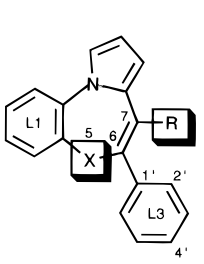

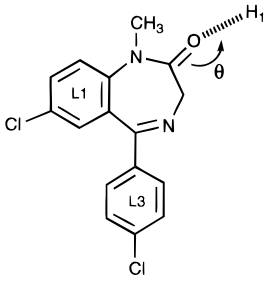

Ro 5-4864

compd	R	X	torsional angles (deg)	θ (deg)	L1-L3 (Å)	H1-L1 (Å)	H1-L3 (Å)
17c	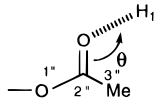	O	τ(6,7,1",2") = 154 τ(7,1",2",3") = 176	130	5.8	6.5	7.7
17e	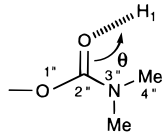	O	τ(6,7,1",2") = 145 τ(7,1",2",3") = 161 τ(1",2",3",4") = 175	130	5.7	6.5	7.5
17d	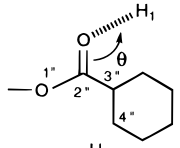	O	τ(6,7,1",2") = 144 τ(7,1",2",3") = 170 τ(1",2",3",4") = 32	140	5.8	6.5	7.6
19	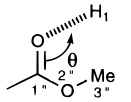	O	τ(6,7,1",2") = -51 τ(7,1",2",3") = 180	220	5.7	6.1	6.4
20	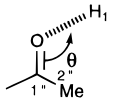	O	τ(6,7,1",2") = -48	220	5.7	5.9	6.3
22	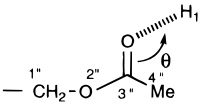	O	τ(6,7,1",2") = 43 τ(7,1",2",3") = 81 τ(1",2",3",4") = 180	180	5.7	6.4	7.7
5d[a]	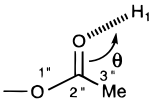	S	τ(6,7,1",2") = 155 τ(7,1",2",3") = 178	140	6.3	6.1	7.9
5g	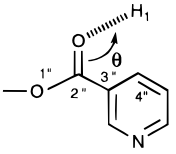	S	τ(6,7,1",2") = 160 τ(7,1",2",3") = 170 τ(1",2",3",4") = 172	150	6.1	5.9	8.1
Ro 5-4864				210	4.9	6.5	8.0

[a] **5d** is substituted with a chlorine atom at the 4′-position.

ed system of aromatic residues and an electron-rich site of the PBR. The lower potency of **17d** with respect to **17c** might result, to a lesser extent, from a nonoptimal steric complementarity between the relatively rigid cyclohexane moiety and the receptor.

Pyrrolobenzoxazepines 17c,e,f, 19, 20, and 22: Effect of Modifications at Position 7 on the Hydrogen Bonding with the Receptor Binding Site (H1). In a recent paper[40] we have proposed the relative 3D location of a hypothetical receptor protic function (H1 site) donating a vital hydrogen bond to a carbonyl or sulfonyl oxygen of the 7-substituent (see Chart 2). This H1 locus was placed at about 2 Å from the acceptor oxygen, 6.0−6.5 Å from the L1 site and 7.8−8.2 Å from the L3 site. To assess the predictive ability of our 3D pharmacophore model, we prepared compounds **19**, **20**, and **22**. While all the so far reported[19,40,53] active pyrrolobenzothiazepines and pyrrolobenzoxazepines feature a 7-OCOR or 7-OSO_2R side chain, **19**, **20**, and **22** bear the 7-CO_2Me, 7-COMe, and 7-CH_2OCOMe groups, respectively. These new 7-substituents were expected to broaden the spectrum of steric and conformational properties in our data set so as to permit a more accurate definition of the 3D pharmacophoric requirements. Figure 3 shows the overlapping active conformations of **19**, **20**, **22**, and **17c**.

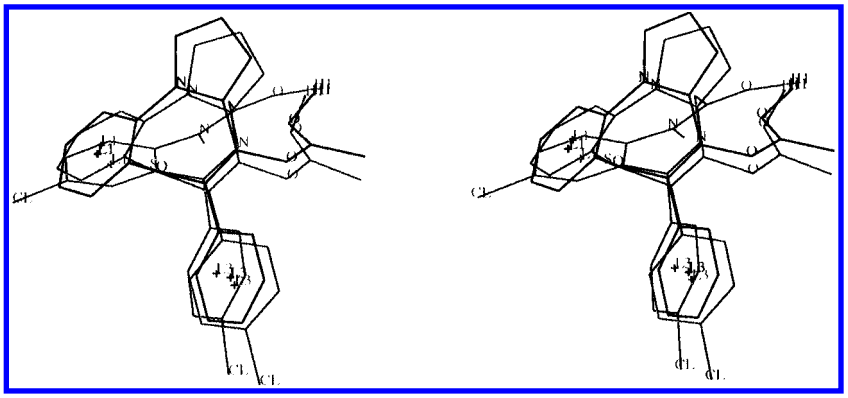

Figure 1. Stereopair picture of the active conformations of **17c** (black) and **5d** (blue) overlapped on the template Ro 5-4864 (red) about the H1, L1, and L3 pharmacophoric points.

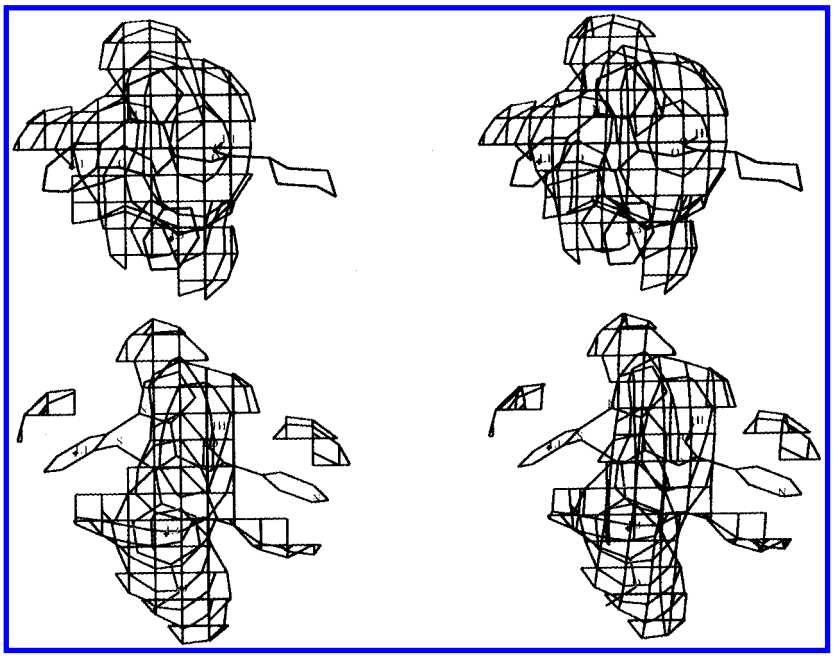

Figure 2. Stereopair picture of the conformations of **17d** (black) and **5g** (red) consistent with the pharmacophore model. Electrostatic potentials (blue) are contoured at the −5 kcal/mol level.

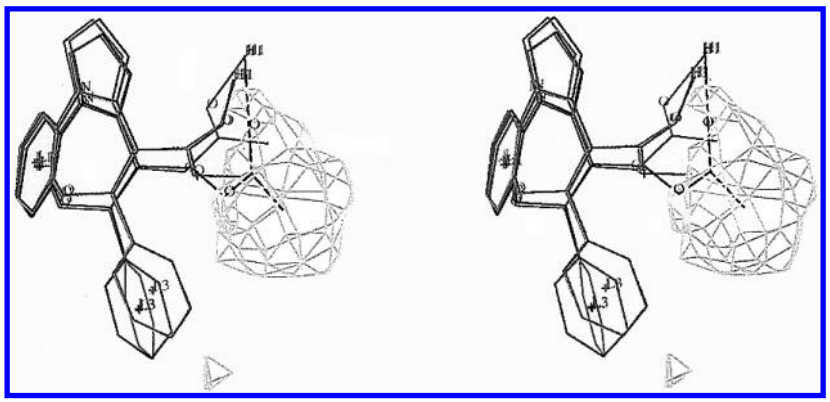

Figure 3. Stereopair picture of the superimposed pharmacophore-consistent conformations of **17c** (green), **19** (blue), **20** (red), and **22** (black). The yellow contour highlights the extra-volume of **22** hypothesized to interfere sterically with the binding to the PBR.

The H1−L1 and H1−L3 distances in **19** and **20** do not exactly match those of **17c** (see also Table 7). However, an average distance deviation of about 0.7 Å was considered still compatible with appreciable affinity. The moderate potency of these two compounds confirmed our predictions. In contrast, **22** fits exactly the pharmacophore geometry. Subsequent testing of **22** showed that this compound exhibits only micromolar affinity. Probably, although the pharmacophoric elements in **22** are correctly oriented in the space, a portion of this ligand experiences steric repulsion within the binding cavity. To test this hypothesis, molecular volume manipulations were performed on the structures of **22** and of the active ligands Ro 5-4864, **17c**, **17e**, **17f**, **19**, and **20** superimposed about the H1, L1, and L3 points. By subtracting the union volume of the above listed active compounds from the volume of **22**, we generated the chickenwire contours depicted in Figure 3 (for sake of clarity, Ro 5-4864, **17e**, and **17f** are not shown). The highlighted extra-volume, surrounding

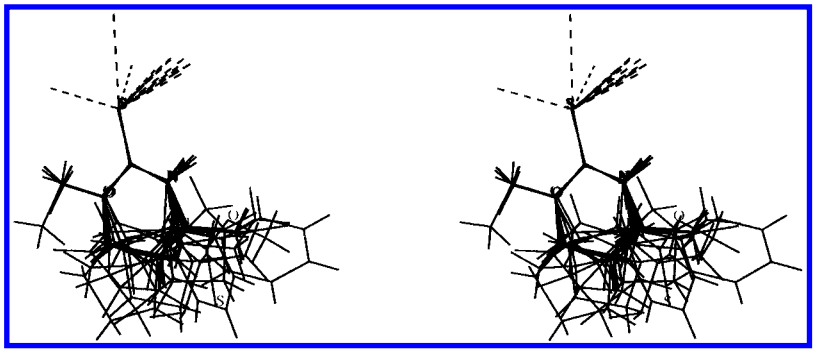

Figure 4. Stereopair picture showing crystal structures of compounds containing the thiocarbamoyloxy fragment. Dashed lines correspond to intermolecular hydrogen bonds accepted by the sp^2-sulfur of the considered fragment.

mostly the terminal methyl group of **22**, corresponds to the locus hypothesized to interfere sterically with the binding. The difference between the IC_{50} values of **19** and **20** can be understood in the light of the work of Raevsky *et al.*[51] who parametrized the hydrogen bonding abilities for a large number of molecules. According to the Raevsky's scale of "proton acceptor free energy factors" (C_a descriptor) the carbonyl oxygen of methyl acetate is a worse hydrogen bond acceptor than that of acetone (C_a values of 1.60 and 2.03, respectively). Replacing the 7-COMe substituent of **20** with a 7-COOMe group so as to give **19** might be considered analogous to converting acetone into methyl acetate. Hence, the lower affinity of **19** with respect to **20** would be the consequence of a weaker hydrogen bond formed between **19** and the H1 receptor site. In the same compilation, the large C_a value assigned to *N*,*N*-dimethylacetamide (2.99) seems also consistent with the hypothesis that the 7-(dimethylcarbamoyl)oxy is more effective than the 7-acetoxy group in accepting a hydrogen bond from the same H1 receptor hydrogen (**17c** *vs* **17e** and **17h** *vs* **17j**).

Of course, the use of the C_a descriptor in structure−affinity relationships is limited to strictly congeneric compounds and requires that other potentially relevant factors (steric, electrostatic, hydrophobic, etc.) are properly taken into account. Following this concept, it is difficult to explain the subnanomolar affinity of the 7-(*N*,*N*-diethylcarbamoyl)oxy derivative **17f** as simply due to a much stronger hydrogen bond interaction. In fact, the C_a value of *N*,*N*-diethylacetamide (3.10) is only 0.11 units above that of *N*,*N*-dimethylacetamide while **17f** is 8 times more potent than **17e**. A possible reason for the remarkably high potency of **17f** is that at least one of the distal methyl groups of the *N*,*N*-diethyl moiety fits optimally a receptor lipophilic region not probed by the ligands tested so far. For simplicity we will designate such a hypothetical lipophilic region as L4 site (see Chart 2). However, since the (CO)N−C bonds in **17f** are free to rotate, we are unable to establish the precise relative 3D location of the L4 site.

Pyrrolobenzoxazepine 17g: Effect of Replacement of the C-7 Carbonyl with a C-7 Thiocarbonyl Group. Compound **17g**, formally derived by replacement of the sp^2-oxygen of **17f** with a sp^2-sulfur was prepared to further elucidate the energetics of the interactions at the H1 and L4 sites. The high binding affinity of compound **17g** raised the question of whether the sulfur atom in compounds containing the O−C(=S)N< fragment can effectively accept hydrogen bonds. To address this issue, we performed a substructure-based search in the Cambridge Structural Database (CSD).[49] As summarized in Table 8, thirteen hits were found with intramolecular S···H hydrogen bonds yielding a mean distance of 2.57 Å. In the Tripos force field,[54] the sp^2-S and H atoms begin to repell each other at distances shorter than 2.94 Å. In one entry (confam) the same sulfur is engaged in two hydrogen bonds. Interestingly, the retrieved crystal structures show a hydrogen bond directionality similar to that reported by Murray-Rust and Glusker for >C=O···H interactions.[55] Figure 4 shows the thirteen structures aligned on the common O−C(=S)N< fragment with the S···H hydrogen bonds drawn as dashed lines.

Table 8. Intermolecular Hydrogen Bond Geometries in Crystal Structures Featuring the O−C(=S)N Substructure

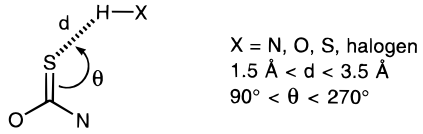

3D query

refcode[a]	*d* (Å)	*θ* (deg)	*τ*(N,C,S,H) (deg)
bumme[b]	2.62	109.9	−5.41
confam[b]	2.68	105.5	10.07
	2.82	247.6	−165.81
dixpab	2.67	111.1	10.56
dojvaz	2.48	108.5	18.12
dojved[c]	2.61	110.8	11.27
	2.66	111.4	−8.51
fezrad	2.89	157.5	40.15
filhaj	2.27	103.0	−6.79
gajroy	2.48	102.4	6.35
keplum[c]	2.30	105.0	−4.41
	2.47	103.2	10.84
kepmat	2.47	106.5	20.56
mescza	2.76	111.4	45.87
pinpil[c]	2.56	108.9	−12.08
	2.50	113.8	−2.28
	2.54	110.4	−4.36
vovwei	2.49	106.2	25.99

[a] Refcode is the reference code of the entry stored in the Cambridge Structural Database (version 5.09); in all the entries X = N. [b] The sulfur accepts two hydrogen bonds. [c] More than one molecule per cell.

The above structural data confirm that the sp^2-sulfur atom of **17g** can accept a hydrogen bond from the H1 receptor site. The particular behaviour of this sulfur probably should be ascribed to a mesomeric effect played the thioamidic nitrogen.

In the Raevsky's compilation[51] the C_a values of *N*,*N*-dimethylthioacetamide and acetone are very close (1.91 and 2.03, respectively).[56] Thus, the free energy involved in the formation of a hydrogen bond with the receptor should be roughly the same for **17g** and **17c**. However, if this was the only relevant factor influencing the affinity, the two compounds should be nearly equipotent.

The IC_{50} value of **17g** (3.8 nM), falling between those of **17c** (12.1 nM) and **17f** (0.7 nM), seems consistent with the hypothesis that one of the *N*-ethyl groups of **17g**, as was previously postulated for **17f**, contributes favorably to the ligand−receptor binding through a direct hydrophobic interaction.

Conclusions

In this paper we have reported the synthesis of a novel class of PBR ligands based on a benzoxazepine skeleton. These compounds showed high affinity and specificity for rat brain PBR and compounds **17f** and **17j** were found to be the most potent PBR ligands to have been identified to date. Some of the most potent compounds were also found to inhibit both [^{3}H]PK 11195 and [^{3}H]Ro 5-4864 binding to the rat adrenal PBR with high affinity (K_i values $\sim$ 1 nM). In order to elucidate the usefulness of such compounds they were screened against one of the proposed roles for the mitochondrial PBR, namely, regulation of steroidogenesis. These highest affinity compounds stimulated steroidogenesis in a mouse Y-1 adrenocortical cell line model with similar potencies and efficacies to each other and to PK 11195 and Ro 5-4864. In view of the high affinity and selectivity of these pyrrolobenzoxazepines for PBR, these compounds represent novel probes for the mitochondrial PBR. They may also be useful in probing the rate-limiting intramembrane transport of cholesterol for steroidogenesis.

Experimental Section

Melting points were determined using an Electrothermal 8103 apparatus and are uncorrected. IR spectra were taken with Perkin-Elmer 398 and FT 1600 spectrophotometers. ^{1}H-NMR spectra were recorded on a Bruker 200 MHz spectrometer with TMS as internal standard; the values of chemical shifts (δ) are given in ppm and coupling constants (J) in Hz. All reactions were carried out in an argon atmosphere. Progress of the reaction was monitored by TLC on silica gel plates (Riedel-de-Haen, Art. 37341). Merck silica gel (Kieselgel 60) was used for chromatography (70−230 mesh) and flash chromatography (230−400 mesh) columns. Extracts were dried over $MgSO_4$, and solvents were removed under reduced pressure. Elemental analyses were performed on a Perkin-Elmer 240C elemental analyzer, and the results are within ±0.4% of the theoretical values, unless otherwise noted. Yields refer to purified products and are not optimized. Physical data for compounds **8**, **9**, **11**, **12**, **14**−**17**, and **19**−**22** are reported in Table 1.

6-Chloro-2-nitrophenol (8). The title compound has been obtained, starting from 2-chlorophenol, following the procedure reported in reference 41. ^{1}H NMR ($CDCl_3$) δ 6.97 (t, 1 H, J = 7.9 Hz), 7.71 (dd, 1 H, J = 7.9, 2.0 Hz), 8.07 (t, 1 H, J = 1.7 Hz), 11.05 (s, 1 H).

1-(3-Chloro-2-hydroxyphenyl)pyrrole (9). To a suspension of **8** (5.0 g, 20 mmol) in ethanol (350 mL) was added a solution of sodium hydrosulfite (20.2 g, 116.3 mmol) in water (93 mL) within 1 h. The resulting mixture was refluxed for 2 h and stirred at rt for 12 h. Then the mixture was filtered, and the filtrate was concentrated. The residue was taken up in EtOAc, dried, and evaporated. Removal of the solvent afforded a residue which was chromatographed (chloroform) to give the corresponding aniline (2.9 g) as a white solid:[41] ^{1}H NMR ($CDCl_3$) δ 3.84 (br s, 2 H), 5.45 (br s, 1 H), 6.60−6.75 (m, 3 H). A pure sample was then tranformed in its hydrochloride salt by mean of 5% methanolic HCl and used in the next step without further purification.

The above hydrochloride salt (0.2 g, 1.1 mmol) was dissolved in boiling water (2 mL) and successively were added sodium acetate trihydrate (0.15 g), boiling glacial acetic acid (4 mL), and 2,5-dimethoxytetrahydrofuran (0.11 mL). After refluxing for 5 min the mixture was rapidly cooled and extracted with EtOAc. The organic layers were washed with 10% sodium hydrogen carbonate solution and brine, dried, and concentrated. The residue was purified by column chromatography (chloroform) to give **9** (0.3 g) as colorless prisms: IR ($CHCl_3$) 3420 cm^{-1}; ^{1}H NMR ($CDCl_3$) δ 5.47 (s, 1 H), 6.37 (m, 2 H), 6.89−7.00 (m, 3 H), 7.20−7.34 (m, 2 H); ^{13}C NMR ($CDCl_3$) δ 109.9, 120.9, 121.4, 121.7, 124.5, 127.5, 129.4, 145.6.

***p*-Azidophenylacetic Acid (11a).** To a solution of 4-aminophenylacetic acid **10** (1.5 g, 10 mmol) in 6 N HCl (20 mL) and concentrated H_2SO_4 (4 mL), cooled at 0 °C, was added sodium nitrite (0.81 g, 12 mmol). After stirring at 0 °C for 30 min, 60 mg of urea were added and the mixture was stirred for an additional 15 min. A solution of sodium azide (1.3 g, 20 mmol) in water (4 mL) was slowly added, and the reaction mixture was stirred at 0 °C for 5 h and then filtered. The solid residue was washed with cold water, dried, and crystallized to give **11a** (1.32 g) as a pale yellow solid: IR (Nujol) 2121, 1695 cm^{-1}; ^{1}H NMR (DMSO-d_6) δ 3.63 (s, 2 H), 7.00 (m, 2 H), 7.25 (m, 2 H).

(±)-α-Bromo-*p*-azidophenylacetic Acid Ethyl Ester (12a). *p*-Azidophenylacetic acid **11a** (0.65 g, 3.7 mmol) was dissolved in anhydrous ethanol (4.6 mL) and a catalytic amount of concentrated H_2SO_4 (30 μL) was added. The reaction mixture was refluxed for 5 h and then concentrated in vacuo. The residue was taken up in dichloromethane, and the organic phase was washed with 10% Na_2CO_3 solution and brine, dried, and evaporated. The oily residue was chromatographed (30% EtOAc in hexanes) to give 0.42 g (56%) of ethyl ester as a solid: mp 40−41 °C (hexanes); IR ($CHCl_3$) 2221, 1720 cm^{-1}; ^{1}H NMR ($CDCl_3$) δ 1.25 (t, 3 H, J = 6.9 Hz), 3.59 (s, 2 H), 4.15 (q, 2 H, J = 6.9 Hz), 7.0−7.25 (m, 4 H). Anal. ($C_{10}H_{11}N_3O_2$) C, H, N.

A mixture of the above ester (0.42 g, 2.05 mmol) and *N*-bromosuccinimide (0.36 g, 20.5 mmol) in carbon tetrachloride (9.5 mL) was refluxed 20 h. The succinimide was filtered off, and the filtrate was concentrated. The residue was directly purified by flash chromatography (toluene) to give the bromo ester **12a** (0.23 g) as a colorless oil: IR (neat) 2220, 1739 cm^{-1}; ^{1}H NMR ($CDCl_3$) δ 1.28 (t, 3 H, J = 7.0 Hz), 4.23 (m, 2 H), 5.31 (s, 1 H), 7.00−7.55 (m, 4 H).

(±)-α-Bromo-*p*-tolylacetic Acid Ethyl Ester (12b). Similarly to the procedure as described for **12a**, the *p*-tolylacetic acid ethyl ester was prepared starting from *p*-tolylacetic acid **11b** (3.0 g, 20 mmol). After chromatography (dichloromethane) the ester (2.95 g, 83%) was obtained as a colorless oil: IR ($CHCl_3$) 1730 cm^{-1}; ^{1}H NMR ($CDCl_3$) δ 1.23 (t, 3 H, J = 7.0 Hz), 2.32 (s, 3 H), 3.56 (s, 2 H), 4.14 (q, 2 H, J = 7.1 Hz), 7.0−7.25 (m, 4 H). Anal. ($C_{11}H_{14}O_2$) C, H, N.

The ethyl ester (1.0 g, 5.6 mmol) was used in the subsequent bromination step to obtain **12b**, as described for **12a**. The bromo ester **12b** was obtained as a colorless oil: IR (neat) 1735 cm^{-1}; ^{1}H NMR ($CDCl_3$) δ 1.27 (t, 3 H, J = 7.5 Hz), 2.34 (s, 3 H), 4.23 (m, 2 H), 5.34 (s, 1 H), 7.14−7.55 (m, 4 H).

(±)-α-[[2-(1*H*-Pyrrol-1-yl)phenyl]oxy]-*p*-tolylacetic Acid Ethyl Ester (14a). Sodium hydride (90 mg, 3.9 mmol) was added to a solution of **13** (0.41 g, 2.6 mmol) in anhydrous THF (5 mL) at rt. The reaction mixture was stirred for 1 h at rt, and then a solution of ethyl α-bromo-*p*-tolylacetate (**12b**) (1.0 g, 3.9 mmol) in anhydrous THF (5 mL) was added dropwise. After 12 h at rt, the solvent was removed in vacuo, and the residue was taken up in dichloromethane. The organic layers were washed with brine, dried, and evaporated. The residue was purified by chromatography (toluene) to give 0.46 g of **14a** as a colorless oil: IR (neat) 1734 cm^{-1}; ^{1}H NMR ($CDCl_3$) δ 1.16 (t, 3 H, J = 7.0 Hz), 2.33 (s, 3 H), 4.13 (q, 2 H, J = 7.0 Hz), 5.48 (s, 1 H), 6.31 (m, 2 H), 6.95−7.40 (m, 10 H).

(±)-α-[[2-(1*H*-Pyrrol-1-yl)phenyl]oxy]-*p*-azidophenylacetic Acid Ethyl Ester (14b). Starting from **13** (0.37 g, 2.34 mmol), the title compound was obtained (reaction time 18 h) following the procedure described for **14a**. After chromatography (toluene), **14b** was obtained as a colorless oil: IR (neat) 2121, 1751 cm^{-1}; ^{1}H NMR ($CDCl_3$) δ 1.16 (t, 3 H, J = 7.0 Hz), 4.14 (q, 2 H, J = 7.0 Hz), 5,47 (s, 1 H), 6.32 (m, 2 H), 6.95−7.44 (m, 10 H).

(±)-α-[[6-Chloro-2-(1*H*-pyrrol-1-yl)phenyl]oxy]phenylacetic Acid Ethyl Ester (14c). Similarly to **14a**, the ester **14c** was prepared starting from 0.5 g (2.6 mmol) of **9** (reaction

time 12 h). **14c** was obtained as colorless oil: IR (neat) 1730 cm^{-1}; ^1H NMR ($CDCl_3$) δ 1.13 (t, 3 H, J = 6.9 Hz), 4.07 (m, 2 H), 4.91 (s, 1 H), 6.32 (m, 2 H), 6.88 (m, 2 H), 6.90−7.30 (m, 8 H).

(±)-α-[[2-(1*H*-Pyrrol-1-yl)phenyl]oxy]-*p*-tolylacetic Acid (15a). The ester **14a** (0.78 g, 2.3 mmol) was dissolved in 26 mL of EtOH/THF mixture (1:1), and 5% aqueous NaOH (22.4 mL) was slowly added. The reaction mixture was stirred at rt for 3 h, concentrated, and acidified with 4 N HCl until pH 3−4. The suspension was extracted with EtOAc, and the organic phase was washed with brine, dried, and concentrated. The residue was crystallized to give the acid **15a** (0.67 g) as colorless prisms: IR (KBr) 1730 cm^{-1}; ^1H NMR ($CDCl_3$) δ 2.32 (s, 3 H), 5.45 (s, 1 H), 6.33 (m, 2 H), 6.90−7.35 (m, 10 H).

(±)-α-[[2-(1*H*-Pyrrol-1-yl)phenyl]oxy]-*p*-azidophenylacetic Acid (15b). Starting from **14b** (0.6 g, 1.65 mmol), the title compound was obtained (reaction time 3 h) following the procedure as for **15a**. After purification by flash chromatography (5% MeOH in EtOAc), **15b** was crystallized as colorless prisms: IR (KBr) 2220, 1730 cm^{-1}; ^1H NMR ($CDCl_3$) δ 5.48 (s, 1 H), 6.30 (m, 2 H), 6.90−7.50 (m, 10 H).

(±)-α-[[6-Chloro-2-(1*H*-pyrrol-1-yl)phenyl]oxy]phenylacetic Acid (15c). Similarly to **15a** the acid **15c** was prepared starting from 100 mg (0.3 mmol) of **14c** (reaction time 3 h). **15c** was obtained as colorless prisms: IR (neat) 3420, 1710 cm^{-1}; ^1H NMR ($CDCl_3$) δ 4.70 (s, 1 H), 5.39 (br s, 1 H), 6.15 (m, 2 H), 6.74−7.26 (m, 10 H).

(±)-6-*p*-Tolylpyrrolo[2,1-*d*][1,5]benzoxazepin-7(6*H*)-one (16a). Phosphorus pentachloride (0.4 g, 1.92 mmol) was added to a solution of acid **15a** (0.58 g, 1.89 mmol) in dry 1,2-dichloroethane (8.5 mL) within 20 min. The reaction mixture was stirred at rt for 5 h and then was poured into crushed ice, basified with 10% NaOH solution, and extracted with chloroform. The organic layers were washed with brine, dried, and evaporated. The residue was chromatographed (dichloromethane and hexanes 2:1) and recrystallized to yield 300 mg of oxazepinone **16a** as colorless prisms: IR ($CHCl_3$) 1640 cm^{-1}; ^1H NMR ($CDCl_3$) δ 2.31 (s, 3 H), 5.50 (s, 1 H), 6.48 (m, 1 H), 7.0−7.40 (m, 10 H).

(±)-6-(*p*-Azidophenyl)pyrrolo[2,1-*d*][1,5]benzoxazepin-7(6*H*)-one (16b). Similarly to **16a**, the oxazepinone **16b** was prepared starting from 0.52 g (1.57 mmol) of **15b** (reaction time 8 h at 30 °C). **16b** was recrystallized as white prisms: IR ($CHCl_3$) 2107, 1648 cm^{-1}; ^1H NMR ($CDCl_3$) δ 5.51 (s, 1 H), 6.51 (m, 1 H), 6.95−7.44 (m, 10 H).

(±)-4-Chloro-6-phenylpyrrolo[2,1-*d*][1,5]benzoxazepin-7(6*H*)-one (16c). Similarly to **16a**, the oxazepinone **16c** was prepared starting from 0.74 g (2.38 mmol) of **15c** (reaction time 10 h at rt). **16c** was obtained as white prisms: IR ($CHCl_3$) 1640 cm^{-1}; ^1H NMR ($CDCl_3$) δ 5.57 (s, 1 H), 6.50 (m, 1 H), 7.09−7.44 (m, 10 H); ^{13}C NMR ($CDCl_3$) δ 90.5, 112.2, 120.6, 121.1, 125.9, 126.3, 128.1, 128.3, 128.6, 129.0, 129.6, 133.5, 135.5, 189.5.

General Procedure for Preparation of Compounds 17a−p. This procedure is illustrated for the preparation of 7-acetoxy-6-ethylpyrrolo[2,1-*d*][1,5]benzoxazepine (**17a**). To a suspension of potassium hydride (0.13 g, 1.1 mmol, 35% in oil) in anhydrous THF (1.5 mL) was added the ketone **16g** (0.25 g, 1.1 mmol) dissolved in anhydrous THF (1 mL). The reaction mixture was stirred at rt for 2 h, and then acetyl chloride (78 μL, 1.1 mmol) was slowly added. After stirring for 12 h at rt, the solvent was removed in vacuo and the residue was taken up in EtOAc. The organic layer was washed with brine, dried, and concentrated. The residue was chromatographed (dichloromethane and hexanes 1:1) to give 196 mg of **17a** as a colorless oil: IR ($CHCl_3$) 1765 cm^{-1}; ^1H NMR ($CDCl_3$) δ 1.21 (t, 3 H, J = 7.2 Hz), 2.22 (s, 3 H), 2.36 (q, 2 H, J = 7.2 Hz), 6.25 (m, 1 H), 6.33 (m, 1 H), 7.06 (m, 1 H), 7.15−7.34 (m, 4 H).

7-[(Dimethylcarbamoyl)oxy]-6-ethylpyrrolo[2,1-*d*][1,5]benzoxazepine (17b). Starting from **16g** (0.25 g, 1.1 mmol) the title compound was obtained according to the procedure described for **17a**, by mean of dimethylcarbamoyl chloride. **17b** was recrystallized as colorless prisms: IR ($CHCl_3$) 1730 cm^{-1}; ^1H NMR ($CDCl_3$) δ 1.23 (t, 3 H, J = 7.0 Hz), 2.40 (q, 2 H, J = 7.0 Hz), 2.93 (s, 3 H), 3.08 (s, 3 H), 6.24 (m, 1 H), 6.32 (m, 1 H), 7.05 (m, 1 H), 7.13−7.35 (m, 4 H).

7-Acetoxy-6-phenylpyrrolo[2,1-*d*][1,5]benzoxazepine (17c). Starting from **16d** (0.2 g, 0.73 mmol), the title compound was obtained according to the procedure as for **17a** and recrystallized as colorless prisms: IR ($CHCl_3$) 1780 cm^{-1}; ^1H NMR ($CDCl_3$) δ 2.19 (s, 3 H), 6.40 (m, 1 H), 7.15−7.39 (m, 10 H), 7.75 (m, 1 H).

7-[(Cyclohexylcarbonyl)oxy]-6-phenylpyrrolo[2,1-*d*]-[1,5]benzoxazepine (17d). Starting from **16d** (0.3 g, 1.08 mmol), the title compound was obtained following the procedure as for **17a**, using cyclohexanecarbonyl chloride. **17d** was recrystallized as pale yellow prisms: IR (Nujol) 1750 cm^{-1}; ^1H NMR ($CDCl_3$) δ 1.11−1.98 (m, 10 H), 2.45 (m, 1 H), 6.37 (m, 1 H), 7.08−7.42 (m, 10 H), 7.56−7.75 (m, 1 H).

7-[(Dimethylcarbamoyl)oxy]-6-phenylpyrrolo[2,1-*d*]-[1,5]benzoxazepine (17e). Similarly to **17a**, the oxazepine **17e** was prepared starting from 0.2 g (0.73 mmol) of **16d** (reaction time 8 h at 30 °C), using dimethylcarbamoyl chloride. **17e** was obtained as white prisms: IR ($CHCl_3$) 1740 cm^{-1}; ^1H NMR ($CDCl_3$) δ 2.93 (s, 3 H), 3.09 (s, 3 H), 6.41 (m, 1 H), 7,10−7.42 (m, 10 H), 7.71 (m, 1 H).

7-[(Diethylcarbamoyl)oxy]-6-phenylpyrrolo[2,1-*d*][1,5]-benzoxazepine (17f). Similarly to **17a**, the oxazepine **17f** was prepared starting from 0.3 g (1.32 mmol) of **16d** (reaction time 6 h at 30 °C), using diethylcarbamoyl chloride. **17f** was obtained as white prisms: IR ($CHCl_3$) 1726 cm^{-1}; ^1H NMR ($CDCl_3$) δ 1.02−1.29 (m, 6 H), 3.27−3.49 (m, 4 H), 6.40 (m, 1 H), 7.06−7.44 (m, 10 H), 7.78 (m, 1 H).

7-[(Diethylthiocarbamoyl)oxy]-6-phenylpyrrolo[2,1-*d*]-[1,5]benzoxazepine (17g). Similarly to **17a**, the oxazepine **17g** was prepared starting from 0.14 g (0.51 mmol) of **16d** (reaction time 12 h at rt), using diethylthiocarbamoyl chloride. **17g** was obtained as pale pink prisms: IR ($CHCl_3$) 1150 cm^{-1}; ^1H NMR ($CDCl_3$) δ 1.25 (m, 6 H), 3.80 (m, 4 H), 6.32 (m, 1 H), 6.40 (m, 1 H), 7.18−7.43 (m, 9 H), 7.79 (m, 1 H); ^{13}C NMR ($CDCl_3$) δ 11.7, 13.7, 44.0, 48.2, 109.5, 110.6, 121.0, 122.0, 122.2, 125.8, 126.7, 126.9, 128.1, 128.3, 128.7, 133.2, 133.6, 135.9, 145.1, 151.8, 185.6; MS m/z 390 (M^+, 20), 313, 281, 246 (100).

7-Acetoxy-6-*p*-tolylpyrrolo[2,1-*d*][1,5]benzoxazepine (17h). Starting from **16a** (0.2 g, 0.69 mmol) the title compound was obtained as colorless prisms, following the procedure as for **17a**: IR ($CHCl_3$) 1760 cm^{-1}; ^1H NMR ($CDCl_3$) δ 2.19 (s, 3 H), 2.37 (s, 3 H), 6.38 (m, 1 H), 7.14−7.39 (m, 9 H), 7.65 (m, 1 H).

7-[(Dimethylcarbamoyl)oxy]-6-*p*-tolylpyrrolo[2,1-*d*][1,5]-benzoxazepine (17i). Similarly to **17a**, the oxazepine **17i** was prepared starting from 0.2 g (0.69 mmol) of **16a** (reaction time 12 h at rt), using dimethylcarbamoyl chloride. **17i** was recrystallized as colorless prisms: IR ($CHCl_3$) 1730 cm^{-1}; ^1H NMR ($CDCl_3$) δ 2.37 (s, 3 H), 2.93 (s, 3 H), 3.09 (s, 3 H), 6.32 (m, 1 H), 6.39 (m, 1 H), 7.13−7.40 (m, 8 H), 7.67 (d, 1 H, J = 8.0 Hz).

7-[(Diethylcarbamoyl)oxy]-6-*p*-tolylpyrrolo[2,1-*d*][1,5]-benzoxazepine (17j). Similarly to **17a**, the oxazepine **17j** was prepared starting from 0.32 g (1.1 mmol) of **16a** (reaction time 8 h at rt), using diethylcarbamoyl chloride and was recrystallized as colorless prisms: IR ($CHCl_3$) 1722 cm^{-1}; ^1H NMR ($CDCl_3$) δ 1.08−1.52 (m, 6 H), 2.37 (s, 3 H), 3.25−3.48 (m, 4 H), 6.32 (m, 1 H), 6.39 (d, 1 H, J = 1.9 Hz), 7.10−7.40 (m, 8 H), 7.65 (d, 1 H, J = 8.25 Hz).

7-Acetoxy-6-(2-naphthyl)pyrrolo[2,1-*d*][1,5]-benzoxazepine (17k). Starting from 0.15 g (0.46 mmol) of **16e**, the title compound was obtained as colorless prisms, following the procedure described for **17a**: IR (Nujol) 1760 cm^{-1}; ^1H NMR ($CDCl_3$) δ 1.83 (s, 3 H), 6.40 (m, 1 H), 6.86 (m, 1 H), 7.10−8.11 (m, 12 H).

7-[(Dimethylcarbamoyl)oxy]-6-(2-naphthyl)pyrrolo-[2,1-*d*][1,5]benzoxazepine (17l). Similarly to **17a**, the oxazepine **17l** was prepared starting from 90 mg (0.27 mmol) of **16e** (reaction time 18 h at 30 °C), using dimethylcarbamoyl chloride. **17l** was obtained as colorless prisms: IR ($CHCl_3$) 1725 cm^{-1}; ^1H NMR ($CDCl_3$) δ 2.61 (s, 3 H), 2.71 (s, 3 H), 6.41 (m, 1 H), 6.88 (m, 1 H), 7.13−8.16 (m, 12 H).

7-[(Dimethylcarbamoyl)oxy]-6-(*p*-azidophenyl)pyrrolo-[2,1-*d*][1,5]benzoxazepine (17m). Starting from 0.16 g (0.51 mmol) of **16b**, the title compound was obtained as a colorless tick oil, using dimethylcarbamoyl chloride, and following the

procedure described for **17a**: IR (neat) 2220, 1725 cm^{-1}; ^1H NMR ($CDCl_3$) δ 2.93 (s, 3 H), 3.11 (s, 3 H), 6.40 (m, 1 H), 7.00−7.40 (m, 9H), 7.77 (m, 1 H).

4-Chloro-7-[(dimethylcarbamoyl)oxy]-6-phenylpyrrolo-[2,1-*d*][1,5]benzoxazepine (17n). Starting from 0.16 g (0.51 mmol) of **16c**, the benzoxazepine **17n** was obtained as colorless prisms following the procedure as described for **17a**, using dimethylcarbamoyl chloride: IR ($CHCl_3$) 1725 cm^{-1}; ^1H NMR ($CDCl_3$) δ 2.94 (s, 3 H), 3.04 (s, 3 H), 6.49 (m, 1 H), 7.05−7.40 (m, 9 H), 7.65−7.76 (m, 1 H); MS *m*/*z* 380 (M^+, 20), 308, 280, 72 (100).

4-Acetoxy-5-phenylnaphtho[2,3-*b*]pyrrolo[1,2-*d*][1,4]-oxazepine (17o). Starting from 0.1 g (0.31 mmol) of **16f**, the title compound was obtained as colorless prisms, following the procedure described for **17a**: IR (Nujol) 1755 cm^{-1}; ^1H NMR ($CDCl_3$) δ 2.20 (s, 3 H), 6.46 (m, 1 H), 7.26 (m, 1 H), 7.38−8.20 (m, 12 H).

4-[(Dimethylcarbamoyl)oxy]-5-phenylnaphtho[2,3-*b*]-pyrrolo[1,2-*d*][1,4]oxazepine (17p). Starting from 0.3 g (0.92 mmol) of **16f**, **17p** was obtained as colorless prisms according to the procedure described for **17a**, using dimethylcarbamoyl chloride: IR ($CHCl_3$) 1725 cm^{-1}; ^1H NMR ($CDCl_3$) δ 2.92 (s, 3 H), 3.09 (s, 3 H), 6.46 (m, 1 H), 7.25−7.84 (m, 13 H).

7-(Methoxycarbonyl)-6-phenylpyrrolo[2,1-*d*][1,5]-benzoxazepine (19). To a suspension of potassium hydride (0.41 g, 3.5 mmol, 35% in oil) in anhydrous DME (5 mL) was slowly added a solution of the benzoxazepinone **16d** (1.0 g, 3.63 mmol) in anhydrous DME (2 mL) under argon. After stirring for 30 min at rt the reaction mixture was cooled at −78 °C and triflic anhydride (0.61 mL, 3.63 mmol) was added. After 1 h at −78 °C, the mixture was allowed to warm to rt. The solvent was removed under vacuum, and the residue, consisting of the *O*-triflate **18**, was dissolved in freshly distilled DMF (15 mL), and palladium diacetate (22 mg, 0.11 mmol), triphenylphosphine (58 mg, 0.21 mmol), and anhydrous MeOH (6.5 mL) were added. The reaction mixture was purged with carbon monoxide and was heated at 50 °C for 2 h under a carbon monoxide atmosphere. After cooling, the solvent was removed under vacuum and the residue was purified by chromatography (30% hexanes in dichloromethane) to give **19** (0.72 g) as pale yellow prisms: IR ($CHCl_3$) 1723 cm^{-1}; ^1H NMR ($CDCl_3$) δ 3.64 (s, 3 H), 6.43 (m, 1 H), 6.53 (m, 1 H), 7.16−7.63 (m, 10 H); ^{13}C NMR ($CDCl_3$) δ 52.4, 111.0, 112.4, 115.4, 121.6, 122.1, 122.9, 126.0, 126.9, 127.1, 127.8, 128.2, 129.5, 133.3, 135.0, 151.4, 155.2, 168.1.

7-Acetyl-6-phenylpyrrolo[2,1-*d*][1,5]benzoxazepine (20). To a solution of ester **19** (100 mg, 0.31 mmol) in anhydrous DME (0.3 mL) cooled at −20 °C was added methyllithium (0.43 mL, 0.688 mmol, 1.6 M solution in diethyl ether). After stirring for 4 h at 0 °C under argon, the reaction mixture was quenched with water (1 mL) and then extracted with diethyl ether. The organic layers were washed with brine, dried, and concentrated. The residue was chromatographed (hexanes and dichloromethane 1:1) to give the ketone **20** (55 mg) as a white solid: IR ($CHCl_3$) 1695 cm^{-1}; ^1H NMR ($CDCl_3$) δ 2.12 (s, 3 H), 6.38 (m, 1 H), 7.13−7.59 (m, 11 H); ^{13}C NMR ($CDCl_3$) δ 31.7, 111.0, 112.3, 121.8, 122.0, 122.9, 123.7, 125.9, 127.1, 127.7, 128.5, 128.5, 129.4, 129.8, 133.3, 134.7, 151.5, 153.0, 202.6.

7-(Hydroxymethyl)-6-phenylpyrrolo[2,1-*d*][1,5]-benzoxazepine (21). To a suspension of LAH (6.6 mg, 0.17 mmol) in anhydrous THF (1 mL) was added the ester **19** (50 mg, 0.17 mmol), and the mixture was stirred for 2 h at rt under argon. After quenching with 10% ammonium chloride solution (1 mL), the mixture was extracted with EtOAc, and the organic layers were washed with brine, dried, and concentrated. The residue was purified by chromatography (dichloromethane) and recrystallized to afford **21** (44 mg) as colorless prisms: IR ($CHCl_3$) 3422 cm^{-1}; ^1H NMR ($CDCl_3$) δ 1.63 (s, 1 H), 4.54 (s, 2 H), 6.46 (m, 1 H), 6.59 (m, 1 H), 7.05−7.67 (m, 10H).

7-(Acetoxymethyl)-6-phenylpyrrolo[2,1-*d*][1,5]-benzoxazepine (22). To a solution of alcohol **21** (15 mg, 0.05 mmol) and dry triethylamine (43 μL, 0.31 mmol) in anhydrous THF (0.3 mL) cooled at 0 °C was added acetyl bromide (15.2 μL, 0.21 mmol). The reaction mixture was stirred at rt for 3 h under argon. After quenching with water (1 mL) the mixture was extracted with EtOAc and the organic phase was washed with brine, dried, and concentrated. The residue was chromatographed (hexanes and dichloromethane 1:1) and recrystallized to give the ester **22** (14 mg) as colorless prisms: IR ($CHCl_3$) 1753 cm^{-1}; ^1H NMR ($CDCl_3$) δ 2.05 (s, 3 H), 4.94 (s, 2 H), 6.42 (m, 1 H), 6.49 (m, 1 H), 7.05−7.60 (m, 10H); ^{13}C NMR ($CDCl_3$) δ 21.0, 63.7, 110.5, 110.7, 114.7, 121.4, 122.1, 122.8, 125.7, 127.0, 128.3, 128.7, 129.1, 129.9, 133.6, 134.9, 151.7, 154.6, 170.9.

Mitochondrial Benzodiazepine Receptor Binding Assay. Male CRL:CD(SD)BR rats (Charles River Italia, Calco, CO, Italy) weighing about 150 g, were used in this experiment. The rats were housed in groups of five in plastic cages, kept under standard conditions (rt 21 ± 1 °C, relative humidity 55 ± 10%, 12−12 h light, dark cycle) and given tap water and food ad libitum. They were decapitated unanesthetized, and the brains were rapidly removed and dissected into anatomically recognizable areas. Cortices were homogenized in about 50 vol of ice-cold phosphate-buffered saline, 50 mM, pH 7.4, using an Ultra Turrax TP 1810 (2 × 20 s) instrument and centrifuged at 50000*g* for 10 min. The pellet was washed three more times by resuspension in fresh buffer and centrifuged as before. The last pellet was resuspended just before the binding assay. For mitochondrial benzodiazepine binding,[57] 10 mg of original wet tissue weight was incubated with 1 nM [^3H]PK 11195 (specific activity 85.8 Ci/mmol; NEN) in 1 mL final volume for 120 min at 4 °C in the presence of 8−12 increasing concentrations of drugs. Nonspecific binding was determined using 1 μM PK 11195. Incubation was stopped by rapid filtration under vacuum through glass fiber filters (Printed Filtermat B, Wallac) which were then washed with 12 mL of ice cold buffer, using a Brandel M48 RP harvester. Filters were put into sample bags with 25 mL of Betaplate Scint (LKB) and counted in a 1204 BS Betaplate liquid scintillation counter, with a counting efficiency of about 45%. IC_{50}s were determined by nonlinear[58] fitting of binding inhibition curves, using the Allifit program running on an IBM AT personal computer. Each point was the mean of triplicate samples.

Adrenal Mitochondrial Preparation and [^3H]PK 11195 and [^3H]Ro 5-4864 Binding. For binding studies, mitochondria were prepared from adrenals of Wistar rats (200−250 g) killed by cervical dislocation. Adrenal glands were removed, homogenized in buffer A (50 mM Tris/Cl, pH 7.4, containing 0.25 M sucrose and 1 mM EDTA) with a Teflon pestle in a glass homogenizer. The homogenate was centrifuged at 600*g* for 10 min, and the resulting supernatant was then centrifuged at 10000*g* for 10 min. The mitochondrial pellet was then suspended in buffer A and centrifuged at 10000*g* for a further 10 min. The resulting washed mitochondrial pellet was resuspended in 50 mM Tris/Cl, pH 7.4, at a concentration of 2 mg protein/mL as determined by the method of Markwell et al.,[59] for use in binding assays. All procedures were performed at 4 °C. Adrenal mitochondria (20 μg of protein) were incubated with either [^3H]PK 11195 (2 nM) or [^3H]Ro 5-4864 (2 nM) (NEN), in 50 mM Tris/Cl, pH 7.4, with a range of concentrations of the tested compounds (0.1 nM−1 μM) dissolved in this buffer containing 0.1% ethanol, in a total volume of 0.5 mL at 4 °C. Total and nonspecific binding in each case was determined in the absence and presence respectively of unlabeled PK 11195 or Ro 5-4864 (1 μM). All samples were incubated in triplicate for 60 min. Assays were terminated by filtration through Whatman glass fiber filters (GF/B, 2.5 cm) using a Brandel cell harvester. Radioactivity trapped on the filters was determined by liquid scintillation counting. The rat adrenal mitochondria express a large number of [^3H]PK 11195 and [^3H]Ro 5-4864 binding sites (77 and 50 pmol/mg), of high affinity (K_d of 1.5 and 2.2 nM, respectively). The IC_{50} and subsequent K_i values for each compound were generated by the use of the computer programs EBDA and LIGAND. Photoaffinity labeling of rat adrenal mitochondria with **17m** was performed as previously described.[60]

Steroid Biosynthesis. Y1 adrenocortical cells were obtained from the European Collection of Animal Cell Culture (Salisbury, UK). They were cultured in Dulbecco's Modified Eagles Medium supplemented with 2 mM glutamine, gentamycin (100 mg/mL), and 10%FCS. Cultures were maintained in a humidified atmosphere of 5% CO_2/95% air at 37 °C. Y1

cells were seeded in 24-well plates at a density of 3×10^5 cells/well in a final volume of 1 mL. Prior to measurement of pregnenolone production, the cells were washed three times with a simple salts medium consisting of 140 mM NaCl, 5 mM KCl, 1.8 mM $CaCl_2$, 1 mM $MgSO_4$, 10 mM glucose, 10 mM HEPES/NaOH, pH 7.4, plus 0.1% BSA. During experiments, cells were incubated with this simple salts medium in an air incubator at 37 °C. In order to measure pregnenolone secreted into the medium, its further metabolism was blocked by the addition of trilostane (5 μM) and SU 10603 (20 μM) (inhibitors of 3β-hydroxysteroid dehydrogenase and 17α-hydroxylase, respectively) to the simple salts medium. The addition of the tested compounds, PK 11195, Ro 5-4864, or clonazepam to the Y1 cells was made by the complete change of the simple salts medium to medium containing the appropriate concentration (40 μM) of compound. The final concentration of ethanol was constant for all the wells within each experiment and did not exceed 0.5% (v/v), a concentration which on its own had no effect on steroid production. At the end of the incubation period (2 h) the cell medium was saved and centrifuged at 1500*g* for 10 min. The amount of pregnenolone secreted into the medium was quantified by radioimmunoassay (RIA) using an antibody obtained from ICN Biochemical Inc. (California), under the conditions described by the manufacturer. Analysis of the RIA data was performed using the Apple Macintosh ASSAYZAP program obtained from Biosoft.

Computational Chemistry. All molecular modeling was performed with use of the software package SYBYL[61] running on a Silicon Graphics Indigo XS24 workstation. Geometry optimizations were realized with the semiempirical quantum-mechanics methods MNDO,[62] AM1,[63] and PM3[64] available in the MOPAC program[65] as well as with the molecular-mechanics SYBYL/Tripos force field.[54] MOPAC was run using default settings and the keyword "MMOK" for compounds containing an amide bond. Tripos energy minimizations were carried out under conditions detailed in a previous article.[40]

Conformational analyses were carried out on PM3-optimized structures of pyrrolobenzoxazepines to identify global minimum conformers and receptor-recognized conformations. The difference in energy between the two types of conformations, calculated with the Tripos force field, provided an estimate of the strain energy introduced in the binding to the receptor. Whenever this energy exceeded the threshold value of 5 kcal/mol the conformation was rejected.

The April 1995 release (3D graphics 5.09 version for UNIX platforms) of the Cambridge Structural Database (CSD)[49] was searched through substructure queries (metallorganics were not considered). Hits from these searches were used to compare experimental versus theoretical geometries of specific fragments.

Molecules were superimposed by minimizing the root mean square distance (rmsd) relative to selected atom pairs using the SYBYL/FIT command. Three pseudoatoms (H1, L1, and L3) were positioned on the structures of the modeled compounds: L1 and L3 are, respectively, centroids of the fused benzene and the pendant phenyl ring whereas H1 is located 2 Å away from the carbonyl oxygen in the plane of the >C═O system. Generation of the structure of Ro 5-4864 is reported in our previous study.[40]

Choice of the Geometry-Optimization Method for Pyrrolobenzoxazepine Derivatives. A substructure search in the CSD was performed to detect compounds featuring an oxepine ring or any corresponding isosteric ring resulting from CH/N replacements. For this purpose we used the CSD/QUEST graphical routine. Table 9 lists the resulting eleven hits' reference codes and some geometric parameters of the seven-membered rings. Only the tbpoxz entry is a 1,3-oxazepine derivative whereas the remaining compounds contain an oxepine nucleus. All the retrieved crystal structures show a high degree of similarity about the oxygenated cycle. This latter assumes a boat conformation with stern and bow angles falling within intervals of 46−63° and 24−40°, respectively (stern and bow angles are defined in the legend of Table 9).

The Tripos, MNDO, AM1, and PM3 methods were applied to energy-minimize the input crystal structure of cofpoc10 (2,7-diphenyloxepine), selected among the entries in Table 9 for its structural simplicity and high resolution (R = 0.056). Our calculations showed that the PM3 method is the best parametrized for reproducing the geometries of the oxepine ring (see results in Table 9) and hence, we inferred, the most reliable for generating molecular models of pyrrolobenzoxazepines. This inference is supported by the observation that the recently reported[40] crystal structures of the pyrrolobenzothiazepine derivatives **5c**, **5d**, and **5g** (see Table 4) and of 2,7-di-*t*-butylthiaphenine (reference code bikset in the CSD) could be satisfactorily overlapped about the non-hydrogen atoms of their sulfurated seven-membered rings with rmsd values within 0.102 Å. In other words, the hypothesis that oxepine and 1,4-oxazepine rings are geometrically similar relies on the observation that the corresponding isosteric thiaphenine and 1,4-thiazepine rings are indeed similar. Incidentally, the PM3 method performed well in reproducing the geometry of the pyrrolobenzothiazepine system of **5c**, **5d**, and **5g**. The fitting of experimental and PM3 geometries about the fourteen non-hydrogen atoms of the tricyclic nucleus gave rmsd values within 0.091 Å.

Table 9. Geometric Descriptors of Crystallographic and Calculated Structures of Derivatives of Oxepine, 1,3-Oxazepine, and 1,4-Oxazepine

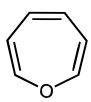

fragment contained in cofpoc10-sixpuc

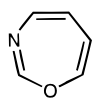

fragment contained in tpboxz

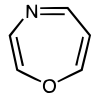

fragment contained in **17c** and **17e**

refcode[a]	C−O(S) (Å)[b]	C−O(S)−C (deg)	stern angle (deg)[c]	bow angle (deg)[d]	rmsd (Å)[e]
cofpoc10	1.41	108.94	60.88	24.42	0.000
bebsoq	1.43	111.14	62.84	28.56	0.057
cufjiw10	1.40	105.10	56.84	40.21	0.098
donvor	1.40	109.92	56.74	25.92	0.022
foltop	1.39	104.72	57.49	39.27	0.101
jasgal	1.41	105.31	59.00	35.54	0.079
peplol	1.39	105.62	57.10	36.03	0.077
sagdot	1.38	115.99	51.56	22.85	0.055
sixpuk	1.38	110.80	45.84	27.22	0.088
tpboxz	1.42	106.88	59.59	30.99	0.061
cofpoc10 (Tripos)	1.34	136.60	2.13	0.28	0.292
cofpoc10 (MNDO)	1.38	120.49	45.52	18.00	0.104
cofpoc10 (PM3)	1.40	111.41	55.62	24.33	0.031
cofpoc10 (AM1)	1.40	112.66	55.30	22.49	0.038
17c (PM3)	1.40	113.52	54.94	28.53	0.053
17e (PM3)	1.40	113.38	53.65	28.59	0.050

[a] Refcode, except for **17c** and **17e**, is the reference code of the entry retrieved from the Cambridge Structural Database (version 5.09); for theoretically derived structures, the geometry-optimization method is reported in parentheses. [b] Mean of two distances. [c] Stern angle is the dihedral angle formed by the plane passing through atoms 2,3,6,7 and the plane passing through atoms 1,2,7 of the seven-membered ring. [d] Bow angle is the dihedral angle formed by the plane passing through atoms 2,3,6,7 and the plane passing through atoms 3,4,5,6 of the seven-membered ring. [e] The rmsd is the root mean square distance resulting from the fitting of each structure on cofpoc10 about the non-hydrogen atoms of the seven-membered ring.

Modeling of 17c and 17e. As a first step, conformers of **17c** and **17e** were constructed by PM3 geometry-optimization of input coordinates derived from the crystal structures of the benzothiazepines **5b** and **5c**.[40] The oxazepine rings of the resulting output structures were found to be nicely superimposable with the oxepine ring of cofpoc10 (see data in Table 9). However, a comparison of the experimental and PM3 optimized structures of **5c** revealed that this semiempirical method did not adequately reproduce the geometry of the 7-$OCON(Me)_2$ substituent. Specifically, in the PM3 geometry the amidic nitrogen is 0.28 Å removed from the plane defined by the three neighboring carbons whereas in the crystal structure this distance is only 0.03 Å. Thus, we decided to mutate **5c** into **17e** by a PM3 partial geometry optimization

which left invariant the geometry of the 7-OCON(Me)$_2$ group. The obtained structures of **17c** and **17e** were assumed to be reasonably close to their global minimum conformers. To find the receptor-recognized conformations of **17c** and **17e**, systematic conformational searches were carried out using the SYBYL/SEARCH routine. Starting from the PM3 global minimum conformer, rotatable bonds about the 7-substituent and the C═O···H1 angle were scanned according to a procedure described in ref 40. Distances H1−L1 and H1−L3 and Tripos energies were recorded in each search run (the L1−L3 distance being invariant). Conformations whose energy was above 5 kcal/mol from the global minimum were rejected. The selected conformations were those which best matched the pharmacophore distances in Ro 5-4864. Both **17c** and **17e** were superimposed on Ro 5-4864 about the H1, L1, and L3 points. The active conformations of Ro 5-4864, **17c** and **5d** are described in Table 7 and shown in Figure 1. Compound **5d** (see Table 4), whose active conformation was directly available from our previous study,[40] was selected as representative of the pyrrolobenzothiazepine series.

Modeling of 17d. A trial model of **17d** was built by replacing the methyl group of the **17c** PM3 global minimum with a cyclohexyl group in a chair conformation. This moiety was retrieved from the SYBYL fragment library.

Two separate conformational analyses on **17d** were carried out with SYBYL/GRIDSEARCH depending on whether the carboxy group was equatorial or axial with respect to the cyclohexane ring. This latter was always in the chair conformation. The rotatable bonds C7−O1″, C2″−C3″, and C6−C1′ (see labels in Table 7) were scanned with 30° steps. The intervals of variation were 0−330° for the first two bonds and 0−150° for the latter bond. In all the minimizations the torsional angle C7−O1″−C2″−C3″ started from a value of 180°. The lowest energy conformation from each search run was energy-minimized with PM3. According to the PM3 calculations, the "equatorial" conformer was about 2 kcal/mol more stable than the "axial" conformer. This result is in agreement with searches performed in the CSD which showed that several crystal structures of carboxycyclohexane derivatives display equatorial arrangements.

We propose for **17d** an active conformation, obtained by manual adjustment of the C7−O1″ and C2″−C3″ rotatable bonds, in which the 7-carboxy moiety overlaps that of **17c** and the cyclohexane ring is oriented equatorially. In such a geometry, the pharmacophoric distances in **17d** are practically coincident with those of **17c** and **17e**, and the cyclohexane shares much of the volume occupied by the 3′-pyridine ring of **5g**. The pharmacophore-consistent conformations of **17d** and **5g** are described in Table 7 and shown in Figure 2.

The hypothesized active conformation of **17d** is consistent with modeling studies recently conducted on a potent pyrrolobenzothiazepine analogue bearing a 7-(morpholin-4′-yl)-carboxy group.[53] Owing to the amidic conjugation, in this compound the morpholine moiety is somewhat coplanar with the carbonyl system and thus oriented in the binding site similarly to the cyclohexane ring of **17d** and the 3′-pyridine ring of **5g**.

Molecular electrostatic potentials for **17d** and **5g**, based on PM3 partial atomic charges (single point calculations), were contoured at −5 kcal/mol through the SYBYL/POTENTIAL routine (see Figure 2).

Modeling of 19, 20, and 22. Starting molecular models for **19**, **20**, and **22** were built by appropriate modifications of the **17c** PM3 global minimum using Tripos standard bond lengths and bond angles. Systematic conformational searches aimed at identifying global minimum energy conformers for **19**, **20**, and **22** were performed using the SYBYL/GRIDSEARCH routine. Energy minimizations were conducted with the Tripos force field. The rotatable bonds C7−C1″, C1′−O2″, and C6−C1′ (see labels in Table 7) were scanned with 30° increments within 0−330° for the first two bonds and within 0−150° for the latter bond. The CO_2Me side chain in **19** was kept fixed with the carbonyl oxygen and the methyl group in a *cis*-like arrangement. Similarly, the methylene fragment and the carbonyl oxygen in **22** were always in a *cis*-disposition. The lowest energy conformation from each search run was successively fully optimized with PM3 to yield the hypothetical global minimum conformers of **19**, **20**, and **22**.

Each of the three PM3 global minima was aligned on the potent analogue **17c** about the non-hydrogen atoms of the common pyrrolobenzoxazepine system and then submitted to a systematic conformational search using the SYBYL/SEARCH routine. In this procedure, the above listed torsion angles and the C═O···H1 angle were scanned through 5° and 10° steps. For each compound we selected a conformation within 5 kcal/mol from the global minimum in which the intermolecular distance between the H1 of the analyzed molecule and the H1 of **17c** was lowest. Such a procedure ensured that the putatively active conformations of **19**, **20**, and **22** could overlap not only about the H1, L1, and L3 points of the template Ro 5-4864 but also about the pyrrolobenzoxazepine skeleton of **17c** and other similar analogues. Results are reported in Table 7 and Figure 3. Molecular volume manipulations were performed using the SYBYL/MVOLUME option to highlight the "extra-volume" of the inactive compound **22** with respect to the active compounds Ro 5-4864, **17c**, **17e**, **17d**, **19**, and **20** (see Figure 3).

Search in the CSD for Hydrogen Bonds Involving the Sulfur of a Thiocarbamoyloxy Moiety. A substructure-based search in the CSD was performed to investigate the hydrogen bond capability of the sp^2-sulfur in compounds containing the O−C(═S)N< fragment. The graphical interface of the CSD/QUEST routine was employed for this purpose. Table 8 lists the 3D query based on the following geometric constraints: S···H distance comprised between 1.5 and 3.0 Å, C═S···H angle comprised between 90° and 270°. Results are listed in Table 8 and shown in Figure 4.

Acknowledgment. This work was supported by grant from MURST (60%) and CNR, Roma.

References

(1) Part of this work has been presented in a preliminary form at the "II Congresso Congiunto Italiano-Spagnolo di Chimica Farmaceutica", (ML19), Aug 30−Sept 3, 1995, Ferrara, Italy.
(2) Braestrup, C.; Squiref, R. F. Specific Benzodiazepine Receptors in Rat Brain Characterized by High-Affinity [^{3}H]Diazepam Binding. *Proc. Natl. Acad. Sci. U.S.A.* **1977**, *74*, 3805−3809.
(3) Regan, J. W.; Yamamura, H. I.; Yamada, S.; Roeske, W. R. High Affinity Renal [^{3}H]Flunitrazepam Binding: Characterization, Localization, and Alteration in Hypertension. *Life Sci.* **1981**, *28*, 991−997.
(4) Schoemaker, H.; Bliss, M.; Yamamura, H. I. Specific High Affinity Saturable Binding of [^{3}H]Ro 5-4864 to Benzodiazepine Binding Site in Rat Cerebral Cortex. *Eur. J. Pharmacol.* **1981**, *71*, 473−475.
(5) Costa, E.; Guidotti, A. Molecular Mechanisms in the Receptor Actions of Benzodiazepines. *Annu. Rev. Pharmacol. Toxicol.* **1979**, *19*, 531−545.
(6) Knapp, R. J.; Malatynska, E.; Yamamura, H. I. From Binding Studies to the Molecular Biology of GABA Receptors. *Neurochem. Res.* **1990**, *15*, 105−112.
(7) Marangos, P. J.; Pate, J.; Boulanger, J. P.; Clark-Rosenberg, R. Characterization of Peripheral-type Benzodiazepine Binding Site in Brain Using [^{3}H]Ro 5-4864. *Mol. Pharmacol.* **1982**, *22*, 26−32.
(8) Benavides, J.; Quartaronet, D.; Imbault, F.; Malgouris, C.; Uzan, A.; Renault, C.; Dubroeucq, M. C.; Gueremy, C.; Le Fur, G. Labeling of "Peripheral-type" Benzodiazepine Binding Site in the Rat Brain by Using [^{3}H]PK 11195, an Isoquinoline Carboxamide Derivative: Kinetic Studies and Autoradiographic Localization. *J. Neurochem.* **1983**, *41*, 1744−1750.
(9) Schoemaker, H.; Boles, R. G.; Horst, W. D.; Yamamura, H. I. Specific High Affinity Binding Site for [^{3}H]Ro 5-4864 in Rat Brain and Kidney. *J. Pharmacol. Exp. Ther.* **1983**, *225*, 61−69.
(10) Saano, V. Affinity of Various for Benzodiazepine Binding Sites in Rat Brain, Heart, and Kidneys in Vitro. *Acta Pharmacol. Toxicol.* **1986**, *58*, 333−338.
(11) Davies, L. P.; Huston, V. Peripheral Benzodiazepine Binding Sites in Heart and Their Interaction with Dipyridamole. *Eur. J. Pharmacol.* **1981**, *73*, 209−211.
(12) Le Fur, G.; Guillox, F.; Rufat, P.; Benavides, J.; Uzan, A.; Renault, C.; Dubroeucq, M. C.; Gueremy, C. Peripheral Benzodiazepine Binding Sites: Effect of PK 11195, 1-(2-Chlorophenyl)-N-methyl-(1-methylpropyl)-3-isoquinoline Carboxamide. II. In Vivo Studies. *Life Sci.* **1983**, *32*, 1849−1856.
(13) Kendall, D. A.; Nahorsky, S. R. Dihydropyridine Calcium Channels Activators and Antagonists Influence Depolarization-Evoked Inositol Phospholipid Hydrolysis in Brain. *Eur. J. Pharmacol.* **1985**, *115*, 31−36.

(14) Olson, J. M.; Ciliax, B. J.; Mancini, W. R.; Young, A. B. Presence of Peripheral-Type Benzodiazepine Binding Sites on Human Erythrocyte Membranes. *Eur. J. Pharmacol.* **1988**, *142*, 47−53.
(15) De Souza, E. B.; Anholt, R. R. H.; Murphy, K. M.; Snyder, S. M.; Kuhar, M. J. Peripheral-Type Benzodiazepine Receptors in Endocrine Organs: Autoradiographic Localization in Rat Pituitary, Adrenal, and Testis. *Endocrinology* **1985**, *116*, 567−573.
(16) Le Fur, G.; Perrier, J.; Uzan, A.; Renault, C.; Dubroeucq, M. C.; Gueremy, C. Peripheral Benzodiazepine Binding Sites: Effect of PK 11195, 1-(2-Chlorophenyl)-N-methyl-(1-methylpropyl)-3-isoquinoline Carboxamide. I. In Vitro Studies. *Life Sci.* **1983**, *32*, 1839−1847.
(17) Almirante, L.; Mugnaini, A.; Rugarli, P.; Gamba, A.; Zefilippo, E.; De Toma, N.; Murmann, W. Derivatives of Imidazole. III. Synthesis and Pharmacological Activities of Nitriles, Amides, and Carboxylic Acid Derivatives of Imidazo[1,2-a]pyridine. *J. Med. Chem.* **1969**, *12*, 122−126.
(18) Kozikowski, A. P.; Ma, D.; Brewer, J.; Sun, S.; Costa, E.; Romeo, E.; Guidotti, A. Chemistry, Binding Affinities and Behavioral Properties of a New Class of "Antineophobic" Mitochondrial DBI Receptor Complex (mDRC) Ligands. *J. Med. Chem.* **1993**, *36*, 2908−2920.
(19) (a) Fiorini, I.; Nacci, V.; Ciani, S. M.; Garofalo, A.; Campiani, G.; Savini, L.; Novellino, E.; Greco, G.; Bernasconi, P.; Mennini, T. Novel Ligands for Mitochondrial Benzodiazepine Receptors: 6-Arylpyrrolo[2,1-*d*][1,5]benzothiazepine Derivatives. Synthesis, Structure−Activity Relationships, and Molecular Modeling Studies. *J. Med. Chem.* **1994**, *37*, 1427−1438. (b) Greco, G.; Novellino, E.; Fiorini, I.; Nacci, V.; Campiani, G.; Ciani, S. M.; Garofalo, A.; Bernasconi, P.; Mennini, T. A Comparative Molecular Field Analysis Model for 6-Arylpyrrolo[2,1-*d*][1,5]benzothiazepines Binding Selectively to the Mitochondrial Benzodiazepine Receptor. *J. Med. Chem.* **1994**, *37*, 4100−4108.
(20) (a) Anholt, R. R. H.; Pedersen, P. L.; De Souza, E. B.; Snyder, S. H. The Peripheral-Type Benzodiazepine Receptor: Localization to the Mitochondrial Outer Membrane. *J. Biol. Chem.* **1986**, *261*, 576−583. (b) Basile, A. S.; Skolnick, P. Subcellular Localization of "Peripheral-Type" Binding Sites for Benzodiazepines in Rat Brain. *J. Neurochem.* **1986**, *46*, 305−308. (c) Hirsch, J. D.; Beyer, C. F.; Malkowitz, L.; Louillis, C. C.; Blume, A. J. Characterization of Ligand Binding to Mitochondrial Benzodiazepine Receptors. *Mol. Pharmacol.* **1989**, *35*, 164−172.
(21) (a) Mestre, M.; Carriot, T.; Belin, C.; Uzan, A.; Renault, C.; Dubroeucq, M.C.; Gueremy, C.; Le Fur, G. Electrophysiological and Pharmacological Characterization of Peripheral Benzodiazepine Receptors in Guinea Pig Heart Preparation. *Life Sci.* **1984**, *35*, 953−962. (b) Grupp, I. L.; French, J. F.; Matlib, M. A. Benzodiazepine RO 5-4864 Increases Coronary Flow. *Eur. J. Pharmacol.* **1987**, *143*, 143−147.
(22) (a) Newman, A. H.; Hogue, B. A.; Basile, A. S.; Hansford, R. G.; Chiang, P. K.; Moreno-Sanchez, R. Inhibition of Oxidative Phosphorylation by Peripheral-Type Benzodiazepines. *FASEB J.* **1989**, *3*, A703. (b) Moreno-Sanchez, R.; Hogue, B. A.; Bravo, C.; Newman, A. H.; Basile, A.S.; Chiang, P. K. Inhibition of Substrate Oxidation in Mitochondria by Peripheral-Type Benzodiazepine Receptor Ligand AHN 086. *Biochem. Pharmacol.* **1990**, *41*, 1479−1484. (c) Larcher, J.-C.; Vayssiere, J.-L.; LeMarquer, F. J.; Cordeau, L. R.; Keane, P. E.; Bachy, A.; Grus, F.; Croizat, B. P. Effect of Peripheral Benzodiazepines Upon the O_2 Consumption of Neuroblastoma Cells. *Eur. J. Pharmacol.* **1989**, *161*, 197−202.
(23) Hirsch, J. D.; Beyer, C. F.; Malkowitz, L.; Beer, B.; Blume, A. J. Mitochondrial Benzodiazepine Receptors Mediate Inhibition of Mitochondrial Respiratory Control. *Mol. Pharmacol.* **1988**, *34*, 157−163.
(24) Wang, J. K. T.; Morgan, J. L.; Spector, S. Benzodiazepines that Bind at Peripheral Sites Inhibit Cell Proliferation. *Proc. Natl. Acad. Sci. U.S.A.* **1984**, *81*, 753−756.
(25) Curran, T.; Morgan, J. I. Superinduction of c-fos by Nerve Growth Factor in the Presence of Peripherally Active Benzodiazepines. *Bioassays* **1987**, *7*, 255−258.
(26) (a) Baulieu, E.-E.; Robel, P. J. Neurosteroids: a New Brain Function? *J. Steroid Biochem. Mol. Biol.* **1990**, *37*, 395−403. (b) Anholt, R. R. H.; De Souza, E. B.; Kuhar, M. J.; Snyder, S. H. Depletion of Peripheral-Type Benzodiazepine Receptors after Hypophysectomy in Rat Adrenal Gland and Testis. *Eur. J. Pharmacol.* **1985**, *110*, 41−46.
(27) Jung-Testas, I.; Hu, Z.; Baulieu, E. E. Biosynthesis of Pregnenolone and Progesterone in Primary Cultures of Rat Glial Cells. *Endocrinology* **1989**, *125*, 2083−2091.
(28) Costa, E.; Guidotti, A. Diazepam Binding Inhibitor (DBI). A Peptide with Multiple Biological Actions. *Life Sci.* **1981**, *49*, 325−344.
(29) Massotti, M.; Slobodiansky, E.; Konkel, D.; Costa, E.; Guidotti, A. Regulation of Diazepam Binding Inhibitor in Rat Adrenal Gland by Adrenocorticotropin. *Endocrinology* **1991**, *129*, 591−596.
(30) Sprengel, R.; Werner, P.; Seeburg, P. Molecular Cloning and Expression of cDNA Encoding a Peripheral-Type Benzodiazepine Receptor. *J. Biol. Chem.* **1989**, *264*, 20415−20421.
(31) McEnery, M. W.; Snowman, A. N.; Trifletti, R. R.; Snyder, S. H. Isolation of the Mitochondrial Benzodiazepine Receptor Associated with the Voltage Dependent Anion Channel and the Adenine Nucleotide Carrier. *Proc. Natl. Acad. Sci. U.S.A.* **1992**, *89*, 3170−3174.
(32) McCauley, L. D.; Park, C. H.; Lan, M. C.; Tonich, J. M.; Shively, J. E.; Gee, K.W. Benzodiazepines and Peptides Stimulate Pregnenolone Synthesis in Brain Mitochondria. *Eur. J. Pharmacol.* **1995**, *276*, 145−143.
(33) Mukhin, A. G.; Papadopoulos, V.; Costa, E.; Krueger, K. E. Mitochondrial Benzodiazepine Receptors Regulate Steroid Biosynthesis. *Proc. Natl. Acad. Sci. U.S.A.* **1989**, *86*, 9813−9816.
(34) Besman, M. J.; Yanagibashi, K.; Lee, T. D.; Kawamura, M.; Hall, P. F.; Shively, J. E. Identification of des-(Gly-Ile)-Endozepine as an Effector of Corticotropin-Dependent Adrenal Steroidogenesis: Stimulation of Cholesterol Delivery is Mediated by the Peripheral Benzodiazepine Receptors. *Proc. Natl. Acad. Sci. U.S.A.* **1989**, *86*, 4897−4901.
(35) Krueger, K. E.; Papadopoulos, V. Peripheral-Type Benzodiazepine Receptors Mediate Translocation of Cholesterol from the Outer to the Inner Membranes in Adrenocortical Cells. *J. Biol. Chem.* **1990**, *265*, 15015−15022.
(36) Purdy, R. H.; Moore, P. H.; Morrow, A. L.; Paul, S. M. The 3a-Hydroxyring A-Reduced Metabolities of Progesterone and Deoxycorticosterone: Natural Ligands of $GABA_A$ Receptors. In *Neurosteroids and Brain Function*; Costa, E., Paul, S. M., Eds.; Thieme Medical Publishers: New York, 1991; Vol. 8, pp 95−101.
(37) Majewska, M. D. Neurosteroids: GABA-Agonists and GABA-Antagonists Modulators of the $GABA_A$ Receptors. In *Neurosteroids and Brain Function*; Costa, E., Paul, S. M., Eds.; Thieme Medical Publishers: New York, 1991; Vol. 8, pp 109−117.
(38) Wu, F.; Gibbs, T. T.; Farb, D. H. Pregnenolone Sulfate: A Positive Allosteric Modulator at the N-Methyl-D-aspartate Receptor. *Mol. Pharmacol.* **1991**, *40*, 333−336.
(39) Romeo, E.; Auta, J.; Kozikowski, A. P.; Ma, D.; Papadopoulos, V.; Puia, G.; Costa, E.; Guidotti, A. 2-Aryl-3-indoloacetamides (FGIN-1) a New Class of Potent and Specific Ligands for the Mitochondrial DBI Receptor. *J. Pharmacol. Exp. Ther.* **1993**, *262*, 971−978.
(40) Dalpiaz, A.; Bertolasi, V.; Borea, P. A.; Nacci, V.; Fiorini, I.; Campiani, G.; Mennini, T.; Manzoni, C.; Novellino, E.; Greco, G. A Concerted Study Using Binding Measurements, X-ray Structural Data, and Molecular Modeling on the Stereochemical Features Responsible for the Affinity of 6-Arylpyrrolo[2,1-*d*][1,5]-benzothiazepines toward Mitochondrial Benzodiazepine Receptors. *J. Med. Chem.* **1995**, *38*, 4730−4738.
(41) Campiani, G.; Nacci, V.; Fiorini, I.; De Filippis, M. P.; Garofalo, A.; Greco, G.; Novellino, E.; Altamura, S.; Di Renzo, L. Pyrrolobenzothiazepinones and Pyrrolobenzoxazepinones: Novel and Specific Non-Nucleoside HIV-1 Reverse Transcriptase Inhibitors with Antiviral Activity. *J. Med. Chem.* **1996**, *39*, 2672−2680.
(42) Katz, L.; Cohen, M. S. Benzoxazole Derivatives. I. 2-Mercaptobenzoxazoles. *J. Org. Chem.* **1954**, *19*, 758−766.
(43) Artico, M.; Porretta, G. C.; De Martino, G. Synthesis of 4*H*-Pyrrolo[2,1-*c*][1,4]benzoxazine. *J. Heterocycl. Chem.* **1971**, *8*, 283−287.
(44) Ethyl p-Tolyl-α-bromoacetate (**12b**) has been already prepared following a different synthetic route than that described in eq 2. See (a) Hoch, J.; Choisy, J. M. Action of Sodamide on α-Bromoarylacetates. *Compt. Rend.* **1959**, *248*, 3314−3316. (b) Salageanu, N.; Sileanu, I. Action of Some Chemical Substances on the Growth of the Roots of Beans. *An. univ. Bucuresti, Ser. Stiint. nat.* **1956**, 135−141. (c) For the preparation of **12c** see reference 19a.
(45) Cacchi, S.; Morera, E.; Ortar, G. Palladium-Catalyzed Carbonylation of Enol Triflates. A Novel Method for One-Carbon Homologation of Ketones to α,*β*-Unsaturated Carboxylic Acids Derivatives. *Tetrahedron Lett.* **1985**, *26*, 1109−1112.
(46) Meinwald, J.; Jensen, C. B.; Lewis, A.; Swithenbank, C. Highly Strained Bicyclic Systems. X. The Chemistry of 6-Substituted *exo*-5-Chlorobicyclo[2.1.1]hexanes. *J. Org. Chem.* **1964**, *29*, 3469−3475.
(47) Papadopoulos, V.; Mukhin, A. G.; Costa, E.; Krueger, K. E. The Peripheral-Type Benzodiazepine Receptor is Functionally Linked to Leydig Cell Steroidogenesis. *J. Biol. Chem.* **1990**, *265*, 3772−3779.
(48) Papadopoulos, V.; Guarneri, P.; Krueger, K. E.; Guidotti, A.; Costa, E. Pregnenolone Biosynthesis in C6−2B Glioma Cell Mitochondria: Regulation by a Mitochondrial Diazepam Binding Inhibitor Receptor. *Proc. Natl. Acad. Sci. U.S.A.* **1992**, *89*, 5113−5117.
(49) Allen, F. H.; Bellard, S.; Brice, M. D.; Cartwright, B. A.; Doubleday, A.; Higgs, H.; Hummelink, T.; Hummelink-Peters, B. G.; Kennard, O.; Motherwell, W. D. S.; Rodgers, J. R.; Watson, D. G. The Cambridge Crystallographic Data Centre: Computer-Based Search, Retrieval, Analysis and Display of Information. *Acta Crystallogr.* **1979**, *B35*, 2331−2339.

(50) Abraham, M. H.; Duce, P. P.; Prior, D. V.; Barratt, D. G.; Morris, J. J.; Taylor, P. J. Hydrogen Bonding. Part 9. Solute Proton Donor and Proton Acceptor Scales for Use in Drug Design. *J Chem. Soc. Perkin Trans. 2* **1989**, 1355−1375.
(51) Raevsky, O. A.; Grigorev, V. Y.; Kireev, D. B.; Zefirov, N. S. Complete Thermodynamic Description of H-Bonding in the Framework of Multiplicative Approach. *Quant. Struct.-Act. Relat.* **1992**, *11*, 49−63.
(52) Hansch, C.; Leo, A.; Unger, S.; Kim, K. H.; Nikaitani, D.; Lien, E. "Aromatic" Substituent Constants for Structure-Activity Correlations. *J. Med. Chem.* **1973**, *11*, 1207−1216.
(53) Nacci V. et al. Unpublished results.
(54) Clark, M.; Cramer, R. D., III; Van Opdenbosch, N. Validation of the General Purpose Tripos 5.2 Force Field. *J. Comput. Chem.* **1989**, *8*, 892−1012.
(55) Murray-Rust, P.; Glusker, J. P. Directional Hydrogen Bonding to sp^2- and sp^3-Hybridized Oxygen Atoms and its Relevance to Ligand−Macromolecule Interactions. *J. Am. Chem. Soc.* **1984**, *106*, 1018−1025.
(56) The C_a values for *N*,*N*-diethylthioacetamide is not reported in ref 50.
(57) Cantoni, L.; Rizzardini, M.; Skorupska, M.; Cagnotto, A.; Categoni, A.; Pecora, N.; Frigo, L.; Ferrarese, C.; Mennini, T. Hepatic Protoporphyria is Associated with a Decrease in Ligand Binding for Mitochondrial Benzodiazepine Receptors in Liver. *Biochem. Pharmacol.* **1992**, *44*, 1159−1164.
(58) Munson, P. G.; Roadbard, D. *Computers in Endocrinology*; Raven Press: New York, 1984; pp 117−145.
(59) Markwell, M.; Haas, S. M.; Bieker, L.; Tolbert, N. A. A Modification of the Lowry Procedure to Simplify Protein Determination in Membrane and Lipoprotein Samples. *Anal. Biochem.* **1980**, *87*, 206−210.
(60) Moynagh, P. N.; Bailey, C. J.; Boyce, S. J.; Williams, D. C. Immunological Studies on the Rat Peripheral-Type Benzodiazepine Acceptor. *Biochem. J.* **1991**, *275*, 419−425.
(61) SYBYL Molecular Modeling System (version 6.01), TRIPOS Ass. St. Louis, MO.
(62) Dewar, M. J. S.; Thiel, W. Ground States of Molecules. 38. The MNDO Method. Approximations and Parameters. *J. Am. Chem. Soc.* **1977**, *99*, 4899−4907.
(63) Dewar, M. J. S.; Zoebish, E. G.; Healy, E. F.; Stewart, J. J. P. AM1: a New General Purpose Mechanical Molecular Model. *J. Am. Chem. Soc.* **1985**, *107*, 3902−3909.
(64) Stewart, J. J. P. Optimization of Parameters for Semi-Empirical Methods. 1. The PM3 method. *J. Comput. Chem.* **1989**, *10*, 209−220.
(65) MOPAC (version 5.00), Quantum Chemistry Program Exchange, No. 455, 1989.

JM960251B